Non-smooth Dynamics Emerging from Predator-driven Discontinuous Prey Dispersal

Joydeb Bhattacharyya (b.joydeb@gmail.com)
Karimpur Pannadevi College https://orcid.org/0000-0003-4600-2776
Joydev Chattopadhyay
ISI: Indian Statistical Institute

Research Article

Keywords: Prey refuge , Intermittent dispersal , Filippov system , Sliding mode dynamics , Sliding bifurcation

Posted Date: May 21st, 2021

DOI: https://doi.org/10.21203/rs.3.rs-473271/v1

Version of Record: A version of this preprint was published at Nonlinear Dynamics on October 13th, 2021.
See the published version at https://doi.org/10.1007/s11071-021-06963-6.

Non-smooth dynamics emerging from predator-driven discontinuous prey dispersal

Joydeb Bhattacharyya · **Joydev Chattopadhyay**

the date of receipt and acceptance should be inserted later

Abstract In ecology, the refuge protection of the prey plays a significant role in the dynamics of the interactions between prey and predator. In this paper, we investigate the dynamics of a non-smooth prey-predator mathematical model characterized by density-dependent intermittent refuge protection of the prey. The model assumes the population density of the predator as an index for the prey to decide on when to avail or discontinue refuge protection, representing the level of apprehension of the prey by the predators. We apply Filippov's regularization approach to study the model and obtain the sliding segment of the system. We obtain the criterion for the existence of the regular or virtual equilibria, boundary equilibrium, tangent points, and pseudo-equilibria of the Filippov system. The conditions for the visibility (or invisibility) of the tangent points are derived. We investigate the regular or virtual equilibrium bifurcation, boundary-node bifurcation and pseudo-saddle-node bifurcation. Further, we examine the effects of dispersal delay on the Filippov system associated with prey vigilance in identifying the predator population density. We observe that the hysteresis in the Filippov system produces stable limit cycles around the predator population density threshold in some bounded region in the phase plane. Moreover, we find that the level of apprehension and vigilance of the prey play a significant role in their refuge-dispersion dynamics.

Keywords Prey refuge · Intermittent dispersal · Filippov system · Sliding mode dynamics · Sliding bifurcation

Mathematics Subject Classification (2000) 92B05 · 92D25 · 92D40

Joydeb Bhattacharyya (✉)

Department Mathematics, Karimpur Pannadevi College, Nadia, West Bengal-741152, India

E-mail: b.joydeb@gmail.com

Joydev Chattopadhyay

Agricultural and Ecological Research Unit, Indian Statistical Institute, Kolkata, West Bengal-700108, India

E-mail: joydev@isical.ac.in

1 Introduction

In an ecosystem, the prey population exhibit a variety of mechanisms to avoid predation [27]. In general, prey prefers to stay away from their predators by utilizing a secondary habitat as refuge protection which is otherwise inaccessible to their predators [34,35]. The prey refuge protection can reduce the predation pressure and subsequently protects the prey population from depletion [15]. Apart from this, a sufficiently large prey refuge can even drive the predator population to extinction [5]. Since refuges are safe for the prey but restrict their foraging time or mating opportunities than in open habitat, there is a reduction in the growth rate in the prey population during refuge [1,18,28,33]. To balance the trade-off between food and safety, prey mostly prefers to stay in the open habitat when the predator population is relatively low and switches to the refuge at a sufficiently high predator population [28]. When the predator population density becomes low, the prey emerges from refuge to take advantage of feeding and mating opportunities in the open habitat [18,28]. In this paper, we investigate the anti-predator behaviour of prey in response to predation risk versus available resources.

The environmental attributes that portray the behaviour of the prey such as habitat usage and foraging strategy are the consequences of natural selection [17]. The behavioural responses of the prey to its predator examine how a prey incorporates the risk of predation in its foraging decisions. The predators create stimuli that alert the target prey of their presence, creating certain apprehension in the prey population [10,11,31]. While different behavioural traits of prey are favoured in different environments, certain behaviour type affects the survival fitness of the prey under the threat of predation [8]. Some prey appears to ignore predator cues when there is a substantial presence of the predators, referred to as bold prey [4,16]. An innately bold prey often stays in the open habitat for a longer period by prioritising resource acquisition at the cost of enhanced predation-driven mortality [16,36], whereas an extremely apprehensive individual being overtly cautious, often overstays in a refuge by missing out the forage and mating opportunities [36]. Regardless of the level of apprehension, some prey may require more information on the predators to make decisions for switching the habitat [14]. In the context of safeguarding against the possible predation, the prey needs some time to ascertain the threat employing vigilance [30]. The vigilance of prey is a behaviour related to monitoring the potential threats caused by their predators. Vigilance can be pre-emptive or reactive. Prey with pre-emptive vigilance is overtly vigilant, whereas, for reactive vigilance, prey chooses a course of action only after the predator density crosses some threshold value. Overt vigilant prey is expected to make faster habitat-choice decisions compared to their less vigilant counterpart.

Prey vigilance is mostly attributed to the apprehension of the prey [20,21,39]. Researchers [2,20] observed that uncertainty in the risk of predation can lead to an increase in the level of vigilance among prey. In an unpredictable environment, apprehensive prey not being able to access the risk of predators, often overestimates the degree of predation risk, thereby increasing their vigilance level. However, the researcher [2] stated that prey vigilance may not always be

an indicator of the state of apprehension. As observed by the researcher [2], in a predictable environment, apprehensive prey when faced by predators with reliably known cues, becomes less vigilant, whereas an unknown cue perceived in a predictable environment will increase the level of vigilance of the prey without any change in prey apprehension. It has also been observed that hunger can keep the vigilance of prey at its low ebb even if the prey is highly apprehensive to its predator [3]. Apart from this, highly apprehensive prey when moving in a group can become less vigilant with an increase in their group size [3]. In this case, we focus on studying the cases when bold prey becomes hypervigilant or highly apprehensive prey becomes less vigilant.

Many researchers have studied prey-predator interactions by assuming that a constant proportion of prey is protected from predation by the refuge [12,13,25,26,37,40]. In reality, the prey dispersal can be density-dependent [23]. To the best of our knowledge, the prey-density-dependent refuge has been studied in relatively few papers [24,29], whereas the study of predator-mediated density-dependent refuge is relatively new. In this paper, we assumed that the prey remains in some open habitat whenever the predator population density is less than some threshold value, representing the loss of prey apprehension when the predators are rare; above the threshold value, a density-dependent refuge of the prey takes place. It seems reasonable to assume that the switching of the habitat of the prey is not instantaneous, rather, there can be some lag due to the prey's behaviour and associated dispersal time. It is important to study the impact of prey behaviour on the dynamics of the system. Here we further modify the model to include the hysteresis effect and an associated switching delay and address the implications of the habitat switching delay in the dynamics of the system. The incorporation of the hysteresis effect in the system allows identifying the level of vigilance of the prey in identifying the threshold population density of the predator.

The main emphasis of our study will be in exploring the dynamic behaviour of the non-smooth system with prey and predator density-dependent refuge and identify the refuge time spent by the prey based on predator-mediated different behavioural responses of the prey.

2 Model equations

In this study, we have considered a two-species predator-prey model in an open habitat under the assumption that a portion of the prey population takes refuge from the predators when the density of the predators goes above a certain threshold level L; below this threshold value, the prey does not go to the refuge and prefers to stay in the open habitat which is more favourable compared to the refuge. The smaller values of L represent prey to be more apprehensive of predation risk, whereas the larger values of L imply that the prey is less scared to predation. Let $x(t)$ and $y(t)$ represent the densities of prey and predator population, respectively at time t in the open habitat. For $y > L$, we assume the

amount of the prey $x_r(t)$ that takes refuge depends on the prey population density in the open habitat at time t given by $x_r(t) = \frac{\alpha x(t)}{\beta + x(t)}$, where α $(0 \leq \alpha \leq 1)$ is the maximum capacity of the refuge and β $(\beta \geq 1)$ is the half saturation coefficient of the refuge. Therefore, the per-capita fraction of prey in the refuge is $0 \leq \frac{x_r(t)}{x(t)} \leq 1$ for all t such that (i) $\lim_{x\to\infty} x_r(t) = \alpha$, (ii) $\lim_{\beta\to\infty} x_r(t) = 0$ and (iii) $\lim_{\alpha\to 0} x_r(t) = 0$.

The prey in the open habitat is assumed to have a logistic growth in the absence of the predators with intrinsic growth rate r and carrying capacity K. In the presence of the predators, the rate of consumption of the prey by the predators is assumed to follow linear functional response with the per-capita consumption rate c. The growth of the predator can be split up into three portions; conversion rate (with conversion efficiency e), density-dependent death rate γ due to intraspecific competition (overcrowding rate), and the natural mortality rate δ.

For $0 < y < L$, the prey prefers to stay in the open habitat. In this case, the equations governing the dynamics are:

$$\begin{aligned} \frac{dx}{dt} &= rx\left(1 - \frac{x}{K}\right) - cxy \\ \frac{dy}{dt} &= ecxy - \gamma y^2 - \delta y, \end{aligned} \tag{1}$$

where $x(0) \geq 0$ and $y(0) \geq 0$.

For $y > L$, a density-dependent refuge protection of the prey is applied. In this case, the density of the prey available for the consumption of the predator in the open habitat at time t is $(x(t) - x_r(t))$, and is governed by the following equations:

$$\begin{aligned} \frac{dx}{dt} &= rx\left(1 - \frac{x}{K}\right) - c\left(1 - \frac{\alpha}{\beta + x}\right)xy \\ \frac{dy}{dt} &= ec\left(1 - \frac{\alpha}{\beta + x}\right)xy - \gamma y^2 - \delta y, \end{aligned} \tag{2}$$

where $x(0) \geq 0$ and $y(0) \geq 0$.

We denote $H(Z) = y(t) - L$ with $Z = (x,\, y)^T \in \mathbf{R}^2_+$, where $\mathbf{R}^2_+ = \left\{Z = (x,\, y)^T : x \geq 0, y \geq 0\right\}$. Therefore, if the predator density falls below the threshold L, that is, $H(Z) < 0$, then the prey stays in the open habitat. If $H(Z) > 0$, then prey starts taking refuge. The mapping $H : \mathbf{R}^2_+ \to \mathbf{R}$ is smooth and the normal vector $H_Z(Z)$ perpendicular to the switching line $\Sigma = \left\{Z \in \mathbf{R}^2_+ : H(Z) = 0\right\}$ is given by $H_Z(Z) = \frac{\nabla H(Z)}{\|\nabla H(Z)\|} = (0, 1)^T$.

A Filippov system [22] with discontinuous right-hand sides given by (1) and (2) can be written as:

$$\dot{Z}(t) = F^{\varepsilon}(Z),\, Z \in S_{\varepsilon} \tag{3}$$

where

$$F^{\varepsilon}(Z) = \begin{pmatrix} rx\left(1 - \frac{x}{K}\right) - c\left(1 - \varepsilon\frac{\alpha}{x+\beta}\right)xy \\ ec\left(1 - \varepsilon\frac{\alpha}{x+\beta}\right)xy - \gamma y^2 - \delta y \end{pmatrix},$$

$$\varepsilon = \begin{cases} 0, \text{ if } y < L \\ 1, \text{ if } y > L, \end{cases}$$

Parameter	Description	Value	Unit	Reference
r	Intrinsic growth rate of x	0.49	year^{-1}	[6]
K	Environmental carrying capacity of x	2.8	no./200m^2	[6]
c	Per capita consumption rate of y	0.22	no.$^{-1}$ 200m^{2}year^{-1}	[6]
e	Conversion efficiency of y	0.5	–	User defined
α	Maximal physical capacity of the refuge	1	no./200m^2	User defined
β	Half saturation coefficient of the refuge	1	no./200m^2	User defined
γ	Overcrowding rate	0.25	no.$^{-1}$ 200m^{2}year^{-1}	User defined
δ	Mortality rate of y	0.1	year^{-1}	[7]

Table 1: Set of parameter values

$S_0 = \{Z \in R^2_+ : H(Z) < 0\}$, $S_1 = \{Z \in R^2_+ : H(Z) > 0\}$, and $Z(0) \geq 0$.

The non-overlapping regions S_0 and S_1 are separated by the switching line Σ such that $S_0 \cup \Sigma \cup S_1 = \mathbf{R}^2_+$. In the region S_0, the prey does not move to the refuge, while in the region S_1, a portion of the prey population goes to the refuge. The switching line Σ divides the system (3) into two subsystems defined in the regions S_0 and S_1. The dynamics of the vector fields $F^\varepsilon(Z)$ $(\varepsilon = 0, 1)$ is analyzed using the classical methods to study systems of ordinary differential equations.

3 Dynamics in the region S_ε $(\varepsilon = 0, 1)$

Clearly, the system (3) has two different structures, a refuge-free system (for $\varepsilon = 0$) and a system with refuge protection for the prey (for $\varepsilon = 1$). First, we show that the solutions of (3) are non-negative and contained in a compact subset of the phase space if the initial values are positive.

From (3) we have $\frac{dx}{dt} = x f^1_{S\varepsilon}(x,y;t)$ and $\frac{dy}{dt} = y f^2_{S\varepsilon}(x,y;t)$, where

$$f^1_{S\varepsilon}(x,y;t) = r\left(1 - \frac{x}{K}\right) - c\left(1 - \varepsilon\frac{\alpha}{\beta + x}\right) y \text{ and}$$

$$f^2_{S\varepsilon}(x,y;t) = ec\left(1 - \varepsilon\frac{\alpha}{\beta + x}\right) x - \gamma y - \delta \ (\varepsilon = 0, 1).$$

Therefore,

$$x(t) = x(0)e^{\int_0^t f^1_{S\varepsilon}(x,y;\tau)d\tau} \text{ and } y(t) = y(0)e^{\int_0^t f^2_{S\varepsilon}(x,y;\tau)d\tau}, \text{ for all } t \geq 0.$$

This gives rise to the following Lemma:

Lemma 3.1 *If $x(0) > 0$ and $y(0) > 0$, then all possible solutions of the system* (3) *are non-negative.*

This implies, all solutions of (3) remains within $\{(x,y) \in \mathbf{R}^2 : x \geq 0, y \geq 0\}$ starting from an interior point of it. Therefore, $\mathbf{R}^2_+ = \{(x,y) \in \mathbf{R}^2 : x > 0, y > 0\}$ is an invariant region, and as long as $x(t) > 0$ and $y(t) > 0$ for all t, the local existence and uniqueness properties hold in $\mathbf{R}^2_+$.

We now prove that the solutions of (3) with initial values in $\mathbf{R}^2_+$ are bounded. From the prey equation we have $\frac{dx}{dt} \leq rx\left(1-\frac{x}{K}\right)$, which implies $x(t) \to K$ as $t \to \infty$ and so, corresponding to $\varepsilon_1 > 0$, there exists $t_{\varepsilon_1} > 0$ such that $x(t) < K+\varepsilon_1$, for all $t \geq t_{\varepsilon_1}$. Thus we get

$$\int_{y(t_{\varepsilon_1})}^{y(t)} \frac{d\xi}{\xi\left(\frac{ec(K+\varepsilon_1)-\delta}{\gamma}-\xi\right)} < \gamma(t-t_{\varepsilon_1}), \text{ which gives } y(t) < \frac{\left(\frac{ec(K+\varepsilon_1)-\delta}{\gamma}\right)y(t_{\varepsilon_1})}{\left(\frac{ec(K+\varepsilon_1)-\delta}{\gamma}-y(t_{\varepsilon_1})\right)e^{-\gamma(t-t_{\varepsilon_1})}+y(t_{\varepsilon_1})}.$$

Therefore, $\lim_{t\to\infty} y(t) \leq \frac{ecK-\delta}{\gamma}$. The following result states the boundedness of the solutions of the system (3).

Lemma 3.2 *All the non negative solutions of the system* (3) *lies in the region*

$$\Gamma = \left\{(x,y) \in R^2_+ : 0 \leq x \leq K,\ 0 \leq y \leq \frac{ecK-\delta}{\gamma}\right\}$$

The results from Lemma 3.1 and 3.2 implies that the system (3) is dissipative.

Next, we find the equilibria of the system (3) and establish the parameter conditions for which stability of the subsystems can be ensured. The system (3) defined in the regions S_ε has the non-trivial nullclines $f^i_{S_\varepsilon} = 0$ ($i = 1,2$ and $\varepsilon = 0,1$) (cf. Fig. 1). We note that if any steady state solution E_{S_ε} of the system (3) lies in S_ε, it becomes a regular equilibrium point, otherwise a virtual equilibrium point. The intersection of the nullclines of the system (3) yields the following equilibria:

(i) The prey-predator-free equilibria $E^0_{S_\varepsilon} = (0,0)$ exist in the region S_0. Since $H(E^0_{S_\varepsilon}) < 0$ ($\varepsilon = 0,1$), the equilibrium $E^0_{S_0}$ is always regular, whereas $E^0_{S_1}$ is always virtual.

(ii) Predator-free equilibria $E^1_{S_\varepsilon} = (K,0)$ always exists in the region S_0. Since $H(E^1_{S_\varepsilon}) < 0$ ($\varepsilon = 0,1$), the equilibrium $E^1_{S_0}$ is always regular, whereas $E^1_{S_1}$ is always virtual.

(iii) The interior equilibrum $E^*_{S_0} = (x^*_0, y^*_0)$ of the system (1) defined in the region S_0 exists if $\delta < ecK$, where $x^*_0 = \frac{K(r\gamma+c\delta)}{ec^2K+r\gamma}$ and $y^*_0 = \frac{r(ecK-\delta)}{ec^2K+r\gamma}$. $E^*_{S_0}$ is regular or virtual according as $y^*_0 < L$ or $y^*_0 > L$ respectively.

The interior equilibrum of the system (2) defined in the region S_1 is $E^*_{S_1} = (x^*_1, y^*_1)$, where x^*_1 is a positive root of the equation

$$r(K-x)(\beta+x) - cK(\beta+x-\alpha)\phi(x) = 0,$$

$$\phi(x) = \frac{(ecx-\delta)(\beta+x)-ec\alpha x}{\gamma(\beta+x)} \text{ and } y^*_1 = \phi(x^*_1).$$

Since the boundary equilibria $E^0_{S_1}$ and $E^1_{S_1}$ the subsystem (2) are always virtual, these have no biological significance and have nothing to do with the dynamics of the system (3). Therefore, by using eigenvalue analysis, we investigate the local behaviour of the subsystems (1) and (2) around the equilibria $E^0_{S_0}$, $E^1_{S_0}$ and $E^*_{S_\varepsilon}$ ($\varepsilon = 0,1$).

The eigenvalues of the Jacobian matrix of the subsystem (1) at $E^0_{S_0}$ are r and $-\delta$. Therefore, $E^0_{S_0}$ is always a saddle point. Since $E^0_{S_1}$ is always virtual, it follows that the organisms of the system (3) are unlikely to go to extinction.

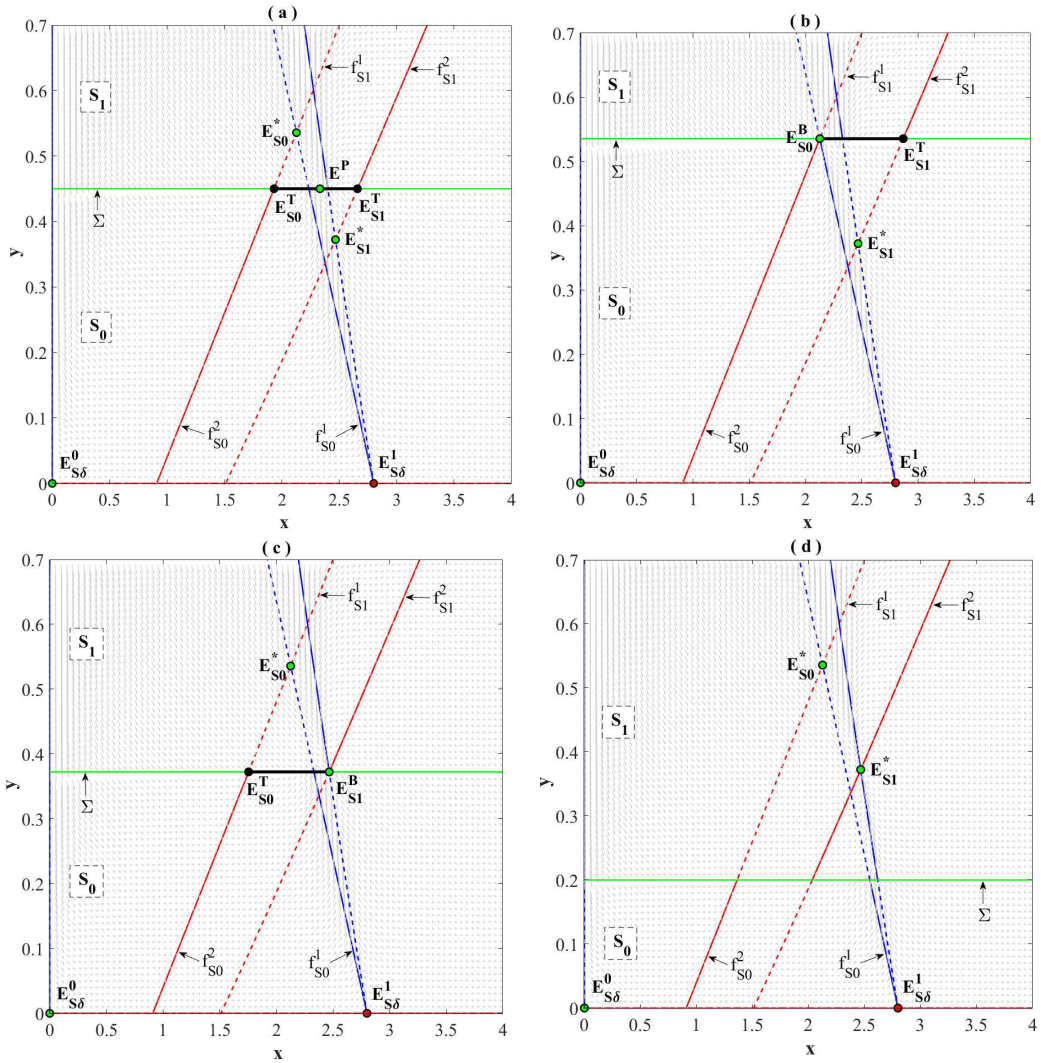

Fig. 1: The positions of the nullclines $(f^i_{S_\varepsilon})$, regular or virtual equilibria, pseudo-equilibrium (E_P), tangent point $(E^T_{S_\varepsilon})$, boundary point $(E^B_{S_\varepsilon})$ and sliding segmant (in black) are shown for (a) $L = 0.3$, (b) $L = y^*_0$ and (c) $L = y^*_1$ $(i = 1,2; \varepsilon = 0,1)$. (d) For $L < y^*_1$, the interior equilibrium $E^*_{S_1}$ becomes regular, whereas $E^*_{S_0}$ is virtual, and so no sliding mode exists. The prey and predator-nullclines are represented by blue and red curves, respectively. The solid blue and red curves represent the nullclines within the domain of definition of the system, whereas the dashed curves represent the position of the nullclines outside their domain of definition.

At $E^1_{S_1}$, the eigenvalues of the Jacobian matrix of the subsystem (2) are $-r$ and $\delta^* - \delta$, where $\delta^* = ecK$. Therefore, the predator-free equilibrium $E^1_{S_1}$ is locally asymptotically stable if $\delta > \delta^*$. This implies, a high mortality rate of the predators can lead to its extinction. The stability at $E^1_{S_1}$ implies the non-existence of $E^*_{S_1}$.

Lemma 3.3 *The system (3) defined in the region S_ε $(\varepsilon = 0,1)$ has no limit cycles.*

Proof We use the Bendixson–Dulac criterion [32] to verify the non-existence of limit cycles in (3). For this, let us consider a Dulac function as follows

$$\Psi(x,y) = \frac{1}{xy}, \text{ where } x \neq 0 \text{ and } y \neq 0.$$

Then,

$$\frac{\partial(f^1_{S_\varepsilon}\Psi)}{\partial x}+\frac{\partial(f^2_{S_\varepsilon}\Psi)}{\partial y} = \frac{\partial}{\partial x}\left\{\frac{r}{y}\left(1-\frac{x}{K}\right)-c\left(1-\varepsilon\frac{\alpha}{\beta+x}\right)\right\}+\frac{\partial}{\partial y}\left\{ec\left(1-\varepsilon\frac{\alpha}{\beta+x}\right)-\frac{\gamma y}{x}-\frac{\delta}{x}\right\}$$
$$= -\frac{r}{yK}-\frac{\gamma}{x}-\frac{c\alpha}{(\beta+x)^2}<0$$

Therefore, the system (3) has no limit cycles and hence the proof is complete.

We note that $E^0_{S_0}$ is always a saddle point and if $\delta<\delta^*$ is satisfied, then the equilibrium $E^1_{S_0}$ is a repeller. Also, the system (3) is dissipative. Therefore, for the persistence of the system (3) at $E^*_{S_\varepsilon}$ $(\varepsilon=0,1)$, we must have $\delta<\delta^*$. Since the system (3) has no periodic solution and is persistent for $\delta<\delta^*$, a sufficient condition for the stability at $E^*_{S_\varepsilon}$ is given by the following Lemma:

Lemma 3.4 *The system (3) defined in the region S_ε is locally asymptotically stable at $E^*_{S_\varepsilon}$ $(\varepsilon=0,1)$ if $\delta<\delta^*$.*

The boundary equilibrium $E^1_{S_0}$ collides with the interior equilibrium $E^*_{S_0}$ when $\delta=\delta^*$ and exchanges stability. Therefore, we investigate the qualitative changes in the dynamic behaviour of the system (3) defined in the region S_0 by varying the parameter δ.

At $\delta=\delta^*$, the Jacobian matrix $J^1_{S_0}$ at $E^1_{S_0}$ has a zero eigenvalue. Thus, at $\delta=\delta^*$, the equilibrium point $E^1_{S_0}$ becomes non-hyperbolic and the usual linearization technique fails to infer the criteria of stability at $E^1_{S_0}$. In the following Lemma we show that under some certain conditions a transcritical bifurcation occurs when δ crosses δ^*.

Lemma 3.5 *If $r\neq cK$, the subsystem* (1) *undergoes a transcritical bifurcation at $E^1_{S_0}$ when δ crosses δ^*.*

Proof The eigenvectors of the subsystem (1) corresponding to the zero eigenvalue for $J^1_{S_0}$ and $J^{1^T}_{S_0}$ are given by $U_1=\begin{pmatrix}-\frac{cK}{r} & 1\end{pmatrix}^T$ and $V_1=\begin{pmatrix}0 & 1\end{pmatrix}^T$ respectively.

At $\delta=\delta^*$, we have $V_1^T F^0_\delta(E^1_{S_0})=0$, $V_1^T\left[\left(DF^0_\delta(E^1_{S_0})\right)(U_1)\right]\neq 0$ if $r\neq cK$ and $V_1^T\left[D^2F^0(E^1_{S_0})(U_1,U_1)\right]=-2\gamma<0$.

Therefore, if $r\neq cK$, the system (3) defined in S_0 satisfies the Sotomayor theorem [32] for transcritical bifurcation at $E^1_{S_0}$ when δ crosses δ^*.

From Lemma 3.5 it follows that if $r\neq cK$ is satisfied, the subsystem (1) switches its stability from $E^*_{S_0}$ to $E^1_{S_0}$ as δ is increased through δ^*. A one-parameter bifurcation plot with δ as a bifurcation parameter is shown in Fig. 2. We observe that, for small values of δ, the equilibrium $E^*_{S_0}$ becomes virtual and $E^*_{S_0}$ is regular and stable. With an increase in δ, the predator population density decreases and once the predator population y_1^* drops below L the regular stable equilibrium $E^*_{S_1}$ becomes virtual. In this case, the system (3) stabilizes at the pseudo-equilibrium E^P_0 on the sliding domain $\Sigma_S\subset\Sigma$ (as defined in section 4) until δ reaches $\delta^*_0=\frac{ercK-L(ec^2K+r\gamma)}{r}$. For $\delta^*_0<\delta<\delta^*$, the system (3) stabilizes at the regular equilibrium $E^*_{S_0}$. For $\delta>\delta^*$, the system (3) becomes stable at the predator-free equilibrium $E^1_{S_0}$ (cf. Fig. 2).

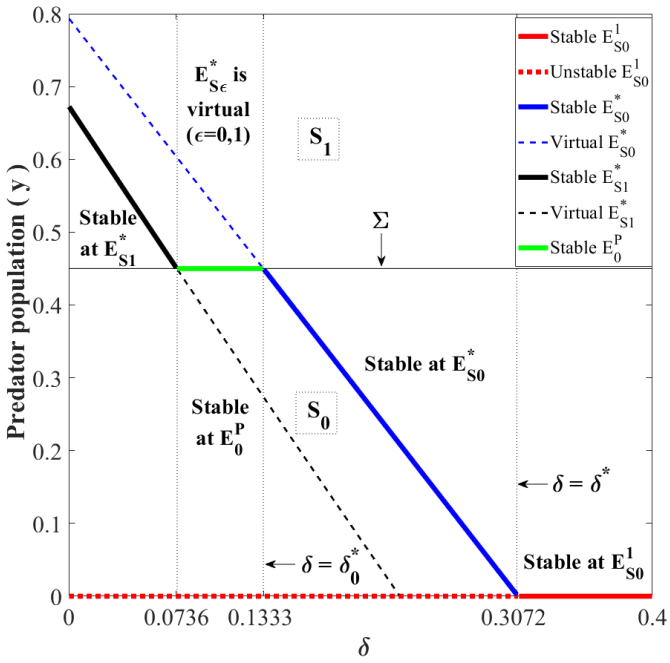

Fig. 2: A one-parameter bifurcation plot for the system (3) with δ as a bifurcation parameter.

In the following section, we discuss about the existence of a sliding domain on the switching boundary and analyze the dynamics of the Filippov system (3) on the sliding domain.

4 Sliding mode on Σ and its dynamics

The system (3) with right hand discontinuity is not defined for $Z \in \Sigma$. To analyze the exhaustive dynamics of the Filippov system (3) on the switching line Σ, we need to employ Filippov's convex method [22] and Utkin's equivalent control method [38] and determine sufficient conditions for the occurrence of a sliding mode on Σ.

By the Lie derivative method, the directional derivative of H along the vector field $F^{\varepsilon}(Z)$, can be written as $L_{F^{\varepsilon}}H(Z) = \langle \nabla H(Z), F^{\varepsilon}(Z) \rangle$ $(\varepsilon = 0,1)$, where $\langle .,. \rangle$ denotes the inner product in $\mathbf{R}^2$.

A sliding mode exists if the vectors $F^{\varepsilon}(Z)$ $(\varepsilon = 0,1)$ on Σ of the two subsystems are pointed towards one another. The sliding domain Σ_S can be expressed as $\Sigma_S = \{Z \in \Sigma : L_{F^0}H(Z) \cdot L_{F^1}H(Z) < 0\} = \Sigma_e \bigcup \Sigma_s$, where $\Sigma_e = \{Z \in \Sigma : L_{F^0}H(Z) < 0 < L_{F^1}H(Z)\}$ is the escaping region and $\Sigma_s = \{Z \in \Sigma : L_{F^1}H(Z) < 0 < L_{F^0}H(Z)\}$ is the sliding region. Since $L_{F^0}H(Z) = L_{F^1}H(Z) + \frac{ec\alpha xL}{\beta + x}$ for all $Z \in \Sigma$, it follows that $\Sigma_e = \phi$. Therefore, the system (3) has no escaping region, the uniqueness of trajectories of (3) is ensured.

The sliding region is given by $\Sigma_s = \{Z \in \Sigma : x_{L_0} < x < x_{L_1}\}$, where

$$x_{L_0} = \frac{\gamma L + \delta}{ec} \text{ and } x_{L_1} = \frac{\alpha - \beta + x_{L_0} + \sqrt{(\alpha - \beta + x_{L_0})^2 + 4\beta x_{L_0}}}{2}.$$

Thus, we have $\Sigma_S = \Sigma_e \bigcup \Sigma_s = \Sigma_s$ and as long as $x_{L_0} < x < x_{L_1}$ holds, any trajectory that hits the sliding segment Σ_S, stays there. The motion on Σ_S represents that the preys are hesitant to take refuge protection.

The crossing region is given by $\Sigma_c = \Sigma_{c-} \bigcup \Sigma_{c+}$, where

$$\Sigma_{c-} = \left\{Z \in \Sigma : 0 \leq x < x_{L_0}\right\} \text{ is the crossing region pointing left to the sliding segment and}$$

$$\Sigma_{c+} = \left\{Z \in \Sigma : x > x_{L_1}\right\} \text{ is the crossing region pointing right to the sliding segment.}$$

On the crossing region Σ_c, one of the vector fields points towards the switching boundary Σ and the other pointing away from Σ.

We use Filippov's convex method to extend the vector field of the system (3). For this, we define $F_S(Z) = (1 - \lambda(Z))F^0(Z) + \lambda(Z)F^1(Z)$, where $0 \leq \lambda(Z) \leq 1$ for each $Z \in \Sigma_S$. Then the sliding vector field $F_S(Z)$ on Σ_S becomes a convex combination of the two vector fields $F^0(Z)$ and $F^1(Z)$ of the subsystems.

The convexification of the system (3) leads to a system of convex differential inclusion

$$\dot{Z}(t) = \begin{cases} F^{\varepsilon}(Z),\ Z \in S_{\varepsilon}\ (\varepsilon = 0, 1) \\ F_S(Z),\ \ Z \in \Sigma_S \end{cases} \tag{4}$$

The existence of solutions of the differential inclusion (4) can be guaranteed in the sense of Filippov.

We note that on the sliding segment Σ_S, $\lambda(Z)$ depends on x only. We re-write the Filippov system (4) and use the equivalent control method [19,38] to determine the sliding mode dynamics on Σ_S as follows:

$$\dot{Z}(t) = F^0(Z) + U_H(Z), \tag{5}$$

where the control function is given by

$$U_H(Z) = \left(\lambda(x)\frac{\alpha cxL}{\beta + x}, -\lambda(x)\frac{e\alpha cxL}{\beta + x}\right)^T.$$

On the sliding plane Σ_S, we have $H(Z) = 0$ and therefore we obtain

$$\dot{H} = H_Z\dot{Z}(t) = ecxL\left(1 - \frac{\alpha\lambda(x)}{\beta + x}\right) - \gamma L^2 - \delta L = 0. \tag{6}$$

Solving for $\lambda(x)$, from (6) we get $\lambda(x) = \frac{(ecx - \gamma L - \delta)(\beta + x)}{ec\alpha x}$.

The governing equations in the sliding region Σ_S, obtained by using the equivalent control method [19,38] is

$$\frac{dx}{dt} = rx\left(1 - \frac{x}{K}\right) - cLx_{L_0} \equiv P(x) \tag{7}$$

In the event that the vector fields $F^0(Z)$ and $F^1(Z)$ of the system (3) point towards Σ, a trajectory hitting Σ is compelled to evolve within the sliding region Σ_S governed by the differential equation (7) along the vector field $F_S(Z)$ until reaching some point on Σ_S where one of the two vector fields $F^0(Z)$ or $F^1(Z)$ changes its direction.

There are several different types of equilibria of the Filippov system (4) that includes regular (or virtual) equilibrium, pseudo-equilibrium, boundary equilibrium, and tangent point. We will focus on studying the dynamics of the system (3) on the sliding segment Σ_S.

The dynamics defined on the sliding segment Σ_S is determined by the differential equation (7), which admits pseudo-equilibrium of the Filippov system (4) (cf. Fig. 4). The pseudo-equilibria $E_i^P = (x_i^P, L)$ $(i = 0, 1)$ of the system (4) satisfies the differential equations (7), where

$$x_{0,1}^P = \frac{K \pm K\sqrt{1 - \frac{4cLx_{L_0}}{rK}}}{2}.$$

The pseudo-equilibrium E_i^P $(i = 0, 1)$ exists on the sliding segment Σ_S if $x_{L_0} \leq x_i^P \leq x_{L_1}$ and $L < L_{SN}$, where $L_{SN} = \frac{-\delta + \sqrt{\delta^2 + er\gamma K}}{2\gamma}$. For $L < L_{SN}$ and $0 < x_i^P < x_{L_0}$ or $x_i^P > x_{L_1}$, the pseudo-equilibrium E_i^P becomes virtual and lies on the crossing segment Σ_c $(i = 0, 1)$. The stability of pseudo-equilibria E_i^P $(i = 0, 1)$ is determined by the differential equation (7) defined at the sliding segment Σ_S.

From (7), we have $\frac{dP(x)}{dx}|_{E_{0,1}^P} = \mp r\sqrt{1 - \frac{4cLx_{L_0}}{rK}}$. This gives the following result:

Lemma 4.1 *(i) For $L < L_{SN}$, the pseudo-equilibrium E_0^P of the system* (4) *is always a saddle point and the pseudo-equilibrium E_1^P is always a pseudo-node.*

(iii) For $L = L_{SN}$, a generic pseudo-saddle-node $E_{SN}^P = \left(\frac{K}{2}, L_{SN}\right)$ of the system (4) *exists.*

A boundary equilibria of the system (4) occurs when an equilibrium point of any one of the two subsytems intersects the switching line Σ. Therefore, the boundary equilibria satisfy $F^\varepsilon(Z) = 0$, $H(Z) = 0$, and are given by $E_{S_\varepsilon}^B = (x_\varepsilon^*, L)$ $(\varepsilon = 0, 1)$. The boundary equilibria $E_{S_\varepsilon}^B$ exist on Σ_S when L approaches the critical value $L = y_\varepsilon^*$ $(\varepsilon = 0, 1)$. The existence of boundary equilibrium of the system (4) is shown in Figs. 4(b) and 4(d).

At the tangent points on Σ_S, one of the vectors $F^0(Z)$ or $F^1(Z)$ is tangent to the discontinuity boundary. The tangent points satisfy the equations $L_{F^\varepsilon} H(Z) = 0$ $(\varepsilon = 0, 1)$ and act as a demarcation between the sliding and crossing regions (cf. Fig. 4). Solving these two equations yields the tangent points $E_{S_\varepsilon}^T = (x_{L_\varepsilon}, L)$ $(\varepsilon = 0, 1)$. The tangent points $E_{S_\varepsilon}^T$ are visible if $L_{F^0}^2 H(Z) < 0$ and $L_{F^1}^2 H(Z) > 0$, where $Z \in \Sigma_S$, $L_{F^1}^2 H(Z) = \langle \nabla (L_{F^\varepsilon} H(Z)), F^\varepsilon(Z) \rangle$ $(\varepsilon = 0, 1)$. In either cases the trajectories of $\dot{Z}(t) = F^\varepsilon(Z)$, $Z \in S_\varepsilon$, passing through the point $E_{S_\varepsilon}^T$ stay in the region S_ε $(\varepsilon = 0, 1)$.

Lemma 4.2 *(i) The tangent point $E_{S_0}^T$ is visible if $L > y_0^*$; (ii) The tangent point $E_{S_1}^T$ is visible if $x_0^P < x_{L_1} < x_1^P$.*

Proof *(i)* We have $\nabla (L_{F^0} H(Z)) = (ecy,\ ecx - 2\gamma y - \delta)^T$.

This yields, $L_{F^0}^2 H(Z) = recxy\left(1 - \frac{x}{K}\right) - ec^2 xy^2 + y\left(ecx - 2\gamma y - \delta\right)\left(ecxy - \gamma y^2 - \delta y\right)$. Therefore, on $Z \in \Sigma$, $L_{F^0} H(Z) = 0$ gives $L_{F^0}^2 H(Z) = ecLx\left\{r\left(1 - \frac{x}{K}\right) - cL\right\}$.

On $Z \in \Sigma$, $L_{F^0}^2 H(Z) < 0$ if $x > K\left(\frac{r - cL}{r}\right)$.

Hence, $E_{S_0}^T$ is visible if $L > y_0^*$.

(*ii*) We have $\nabla\left(L_{F^1}H(Z)\right)=\left(ecy-\frac{ec\alpha\beta y}{(\beta+x)^2},\, ecx\left(1-\frac{\alpha}{\beta+x}\right)-2\gamma y-\delta\right)^T$.

Therefore, on $Z\in\Sigma$, $L_{F^1}H(Z)=0$ gives $L^2_{F^1}H(Z)=cL\left\{1-\frac{\alpha\beta}{(\beta+x)^2}\right\}\left\{erx\left(1-\frac{x}{K}\right)-L(\gamma L+\delta)\right\}$.

Since $0\leq\alpha\leq 1$ and $\beta\geq 1$, we have $0\leq\frac{\alpha\beta}{(\beta+x)^2}<\frac{\alpha}{\beta}\leq 1$. Therefore, on $Z\in\Sigma$, $L^2_{F^1}H(Z)>0$ if $x^2-Kx+cLx_{L_0}=\left(x-x_0^P\right)\left(x-x_1^P\right)<0$, where $x_1^P>x_0^P$.

Hence, $E^T_{S_1}$ is visible if $x_0^P<x_{L_1}<x_1^P$.

In the following section we examine the discontinuity-induced bifurcation followed by the changes in the sliding mode domain.

5 Sliding Bifurcation

Sliding bifurcations of the Filippov system (4) are related mainly to the value of L and on the equilibria of its subsystems. We investigate the sets of regular, virtual and pseudo-equilibrium bifurcations of the system (4) by employing numerical methods.

Bifurcation sets of equilibria

We see that the existence and the type of interior equilibria $E^*_{S_\varepsilon}$ $(\varepsilon=0,1)$ are dependent on δ and L. We define the following three curves for the parameters δ and L:

$\Gamma_1=\{(\delta,L):\Phi_0(\delta,L)=0\}$,

$\Gamma_2=\{(\delta,L):\Phi_1(\delta,L)=0\}$ and

$\Gamma_3=\{(\delta,L):\delta=\delta^*\}$,

where $\Phi_0=\delta-\delta_0^*$ and $\Phi_1=rx_{L_1}\left(K-x_{L_1}\right)-cKLx_{L_0}$.

The three curves Γ_i $(i=1,2,3)$ divide the $\delta-L$ parameter plane into six regions, and the existence or coexistence of stable regular or virtual interior equilibria $E^*_{S_\varepsilon}$ $(\varepsilon=0,1)$ is pointed out in each of the regions (cf. Fig. 3). The curves Γ_1 and Γ_2 are used to determine the relationship between pseudo-equilibrium E_0^P and the sliding line Σ_S given by $x_{L_0}\leq x_0^P\leq x_{L_1}$. The curve Γ_3 is used to study the stability of the equilibria $E^*_{S_0}$ and $E^1_{S_0}$ of subsystem (1). We see that for $0\leq\delta<\min\left\{\delta_0^*,\,\delta^*\right\}$, the equilibrium $E^*_{S_0}$ of the subsystem (1) becomes virtual. For $0\leq\delta<\delta^*$ and $\Phi_1(\delta,L)>0$, the equilibrium $E^*_{S_1}$ of the subsystem (2) becomes virtual. Therefore, for $0\leq\delta<\min\left\{\delta_0^*,\,\delta^*\right\}$ and $\Phi_1(\delta,L)>0$, the equilibria $E^*_{S_\varepsilon}$ $(\varepsilon=0,1)$ become virtual followed by the presence of an attracting sliding region bounded by the curves Γ_1 and Γ_2. The boundary equilibria $E^B_{S_\varepsilon}$ $(\varepsilon=0,1)$ appear on the curves Γ_1 and Γ_2 respectively.

When an ordinary equilibrium of (4) collides with the sliding segment Σ, it gives either an equilibrium transition bifurcation or a non-smooth fold bifurcation. For the equilibrium transition bifurcation, an ordinary equilibrium collides

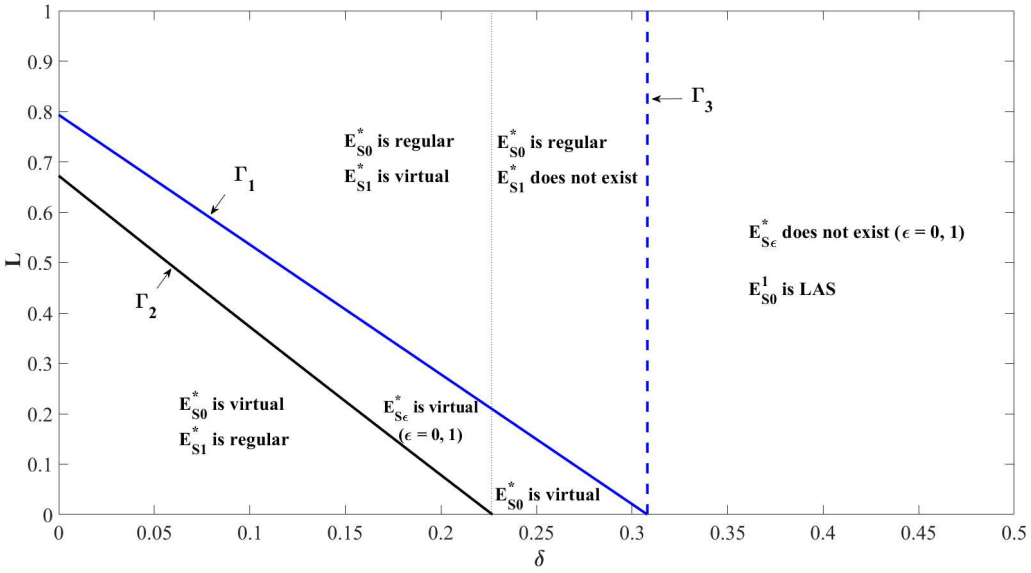

Fig. 3: Two parameter bifurcation diagrams with δ and L as bifurcation parameters. The sliding mode exists in the region bounded by the curves Γ_1 and Γ_2.

with a virtual pseudo-equilibrium, giving rise to a virtual ordinary equilibrium and a pseudo-equilibrium. For the non-smooth fold bifurcation, an ordinary equilibrium collides with a pseudo-equilibrium, giving rise to a virtual ordinary equilibrium and a virtual pseudo-equilibrium.

Boundary equilibrium bifurcation

Boundary equilibrium bifurcation (BEB) in the Filippov system (4) involves the possible topological changes when a real or a virtual equilibrium point collides with the discontinuity boundary Σ due to the changes in some parameter of the system. When $E^*_{S_\varepsilon}$ is a regular equilibrium, a boundary node bifurcation occurs for the system (4) once the tangent point $E^T_{S_\varepsilon}$ and the regular equilibrium $E^*_{S_\varepsilon}$ collides at $L = y^*_\varepsilon$. When $E^*_{S_\varepsilon}$ is a virtual equilibrium, a boundary equilibrium bifurcation occurs when the pseudo-equilibrium E^P_1 and the tangent point $E^T_{S_\varepsilon}$ merge with the equilibrium $E^*_{S_\varepsilon}$ at $L = y^*_\varepsilon$. Therefore, we take L as a bifurcation parameter.

The choice of the values of L is dependent on behavioral pattern of the prey in the presence of the predator. The lower values of L will indicate that the prey is more apprehensive to the predators, whereas the higher value of L indicate that the prey is relatively bold. Under the set of parameter values as given in Table 1, we obtain $E^*_{S_0} = (2.1266,\ 0.5357)$ and $E^*_{S_1} = (2.4669,\ 0.3724)$. From Fig. 4$(a)$ it is observed that for $L < y^*_\varepsilon$ $(\varepsilon = 0, 1)$, the virtual equilibrium point $E^*_{S_0}$, the regular equilibrium $E^*_{S_1}$, the visible tangent point $E^T_{S_1}$ and the invisible tangent point $E^T_{S_0}$ coexist. This indicates that if the prey is very apprehensive to their predators, they will take refuge protection even at a low population density of the predators. In this case, the prey will have to take refuge continuously. Due to this, the predation pressure on the prey will become low, resulting in a high prey population density.

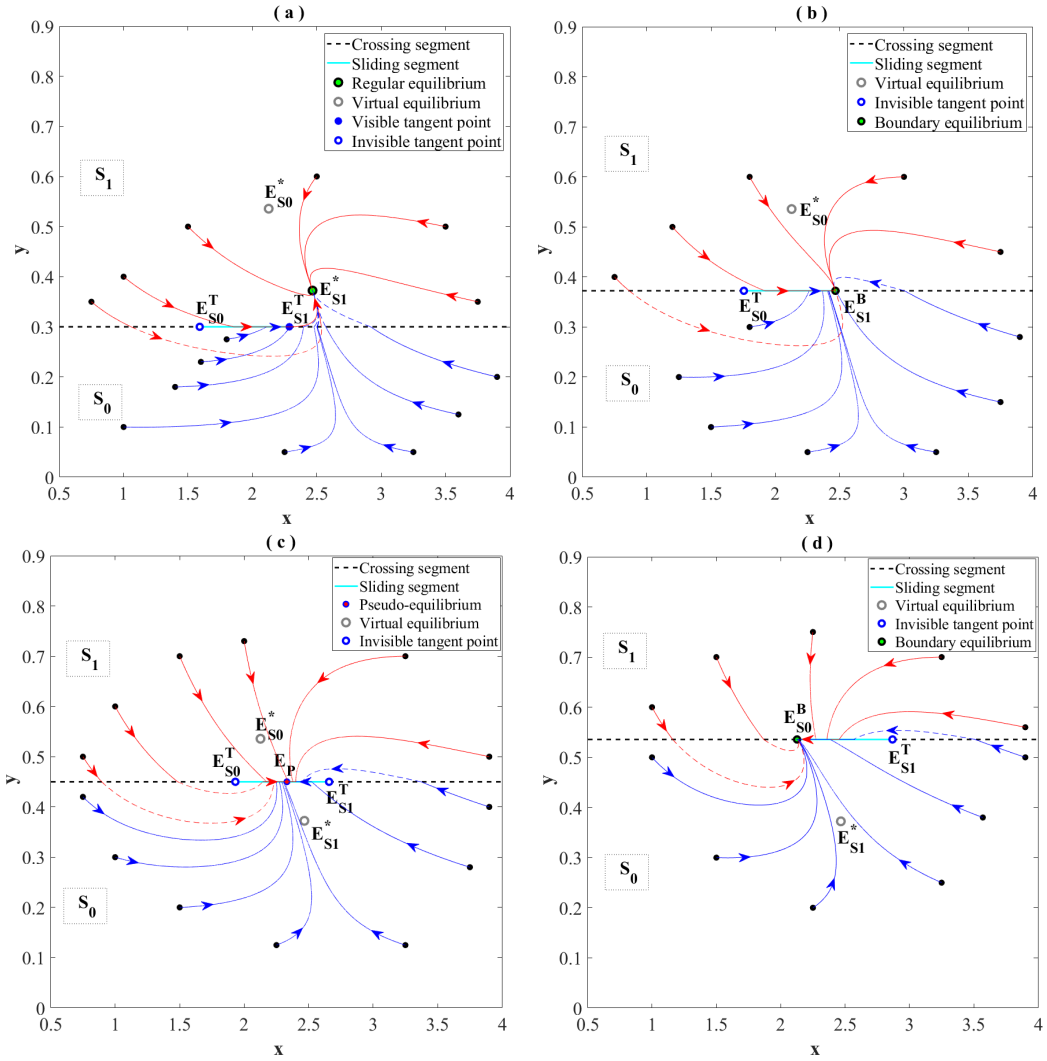

Fig. 4: A boundary node bifurcation with L as a bifurcation parameter for $\delta < \delta^*$. (a) For $0 < L < y^*_\varepsilon$, $E^*_{S_0}$ is virtual and $E^*_{S_1}$ is regular. (b) For $L = y^*_1$, a boundary node bifurcation occurs when $E^*_{S_1}$ merges with the tangent point $E^T_{S_1}$, generating the boundary point $E^B_{S_1}$. (c) For $y^*_1 < L < y^*_0$, E^*_ε becomes virtual followed by the existence of stable pseudo-equilibrium point E^P_1 on the sliding line. (d) For $L = y^*_0$, a boundary node bifurcation occurs when $E^*_{S_0}$ merges with E^P_1 at the boundary point $E^B_{S_0}$ on the switching line.

For relatively bold prey, the threshold population density of the predators to start taking refuge by the prey becomes relatively high. As L is increased through $L = y^*_1$, the stable regular equilibrium $E^*_{S_1}$ collides with the visible tangent point $E^T_{S_1}$, generating the stable boundary equilibrium $E^B_{S_1}$ (cf. Fig. 4(b)). For $y^*_1 < L < y^*_0$, $E^*_{S_\varepsilon}$ becomes virtual $(\varepsilon = 0, 1)$ followed by the emergence of pseudo-equilibrium E^P_1 on the sliding segment (cf. Fig. 4(c)). In this case, both the tangent points $E^T_{S_\varepsilon}$ $(\varepsilon = 0, 1)$ are virtual. In this case, the prey takes refuge protection intermittently and so, the prey-density does not get compromised even with a relatively high population density of the predators. This suggests that the bold prey can prevent their population density from possible depletion even with a high population density of the predators by taking refuge protection intermittently.

Another boundary equilibrium bifurcation of Filippov system (4) occurs when L is increased through $L = y_0^*$. In this case, the virtual equilibrium $E_{S_0}^*$ collides with the pseudo-equilibrium E_1^P at the invisible tangent point $E_{S_0}^T$, generating the stable boundary equilibrium $E_{S_0}^B$ (cf. Fig. $4(d)$). Thereafter, for any further increase of L, the regular equilibrium $E_{S_0}^*$, the virtual equilibrium $E_{S_1}^*$, and the visible tangent point $E_{S_0}^T$ coexist, whereas the pseudo-equilibrium E_1^P disappears from the sliding segment. This indicates that the bold prey (the prey that does not take refuge protection even at a high population density of the predators) is mostly prone to sustained loss in their population driven by high predation pressure.

In order to show the changes in the sliding mode domain with the changes in L and δ, we plot a codimension two bifurcation diagram with L and δ as bifurcation parameters (cf. Fig. $5(a)$). The bifurcation plot confirms the possible existence of a shorter sliding mode domain when the prey is bold and mortality rate of the predator is low. For a more apprehensive prey, a relative larger sliding domain can exist for high mortality rate of the predators. To investigate the sensitivity of the parameters L, c, δ and K for the existence of a pseudo-equilibrium on the sliding domain, we plot bifurcation diagrams as given in Figs. $5(b-d)$. From Figs. $5(b)$ and $5(c)$ it follows that the interval of existence of the pseudo-equilibrium increases with the decrease of the predation rate, while from Fig. $5(d)$ we see that an increase of the prey carrying capacity can lead to longer sliding domain even with low apprehension of the prey.

Pseudo-saddle-node bifurcation

The existence of a pair of pseudo-equilibria on the sliding segment and their subsequent annihilation due to the changes in some threshold parameter values occurs via a saddle-node bifurcation.

Taking $K = 8$ and L as a bifurcation parameter, we observe that a generic pseudo-saddle-node E_{SN}^P appears on the sliding segment Σ when L crosses the critical value $L_{sn}^K = 1.2142$ (cf. Fig. $6(b)$ and Fig. $6(d)$). For $L < L_{sn}^K$, a pseudo-saddle E_0^P and a pseudo-node E_1^P appear on the sliding segment Σ_S (cf. Fig. $6(a)$). In this case, the orbits initiating from $I_{S_0}^0 = (4.05, 1.165)$ and $I_{S_1}^0 = (3.9, 1.25)$ converge to the pseudo-node E_1^P from the left, whereas the orbits initiating from $I_{S0}^1 = (4.25, 1.117)$ and $I_{S_1}^1 = (4.2, 1.25)$ converge to the pseudo-node E_1^P from the right. All the orbits plotted in Fig. $6(a)$, initiated from the left of $I_{S_0}^0$ and $I_{S_1}^0$, converge to the stable regular equilibrium $E_{S_0}^*$. At $L = L_{sn}^K$, the generic pseudo-saddle-node E_{SN}^P is half stable. The orbits starting from $I_{S_0}^0$ and $I_{S_1}^0$ converge to the regular equilibrium $E_{S_0}^*$, whereas, orbits starting from $I_{S_0}^1$ and $I_{S_1}^1$ converge to the pseudo-saddle-node E_{SN}^P from the right (cf. Fig. $6(b)$). For $L > L_{sn}^K$, pseudo-equilibrium does not exist (cf. Fig. $6(c)$ and Fig. $6(d)$) and the regular equilibrium $E_{S_0}^*$ becomes globally asymptotically stable. The effect of L on the variation of the sliding mode is shown in Fig. $6(c)$ and Fig. $6(d)$.

Next, we choose $\gamma = 0.015$ and fix all other parameters as in Table 1. By varying L, for $L < L_{sn}^\gamma = 1.4148$, it is observed that a pseudo-saddle E_0^P close to the tangent point $E_{S_0}^T$ and a pseudo-node E_1^P coexist on Σ_S (cf. Fig. $7(a)$ and Fig. $7(c)$). As L is increased through the critical value $L = L_{sn}^\gamma$, E_0^P and E_1^P collide and generate the pseudo-saddle-node E_{SN}^P (cf. Fig. $7(b)$). As L is increased further, the pseudo-saddle-node E_{SN}^P disappears (cf. Fig. $7(c)$) and the regular

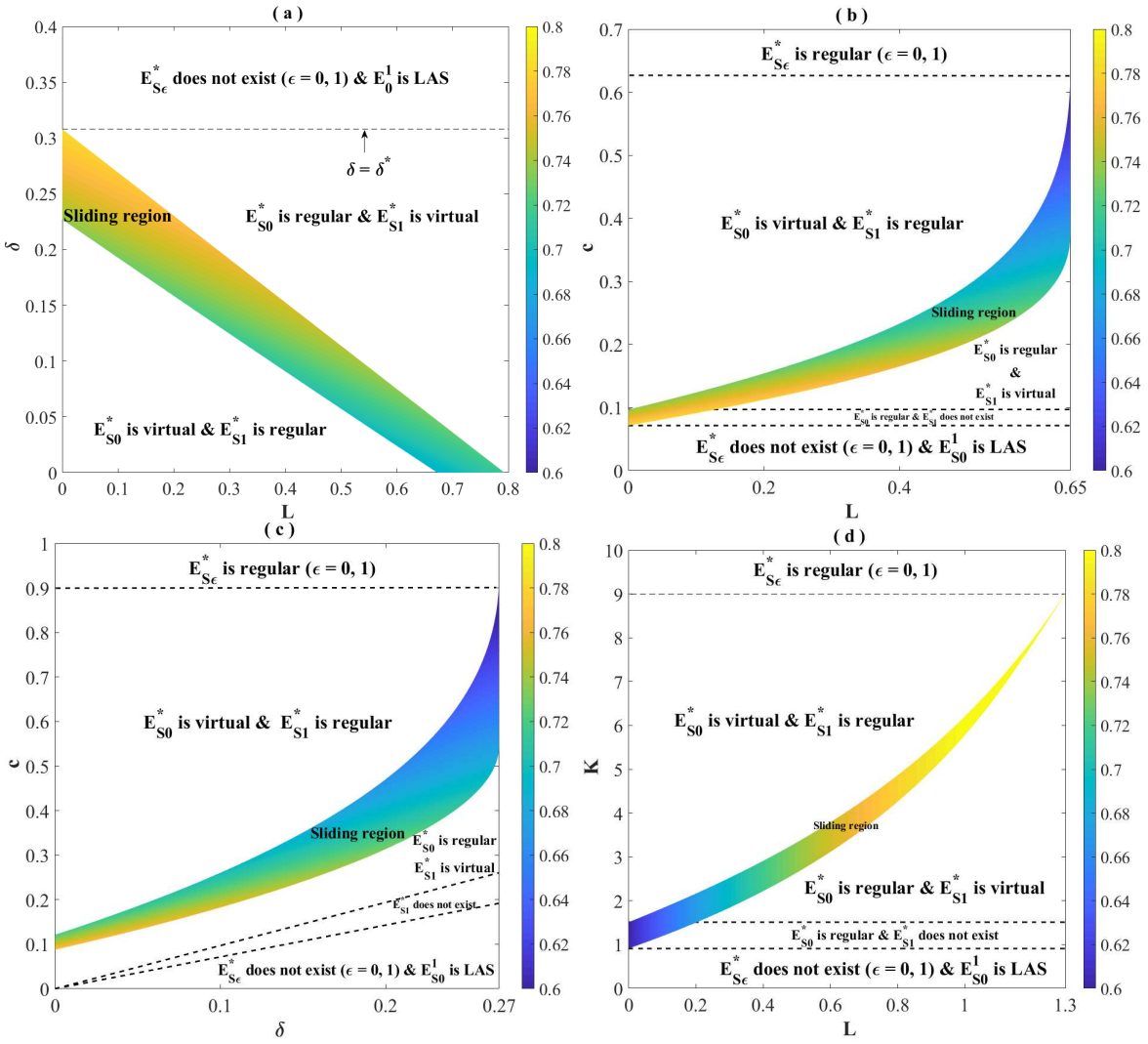

Fig. 5: Sliding mode bifurcation of the Filippov system (4) representing that the sliding mode as a function of (a) L and δ; (b) L and c; (c) δ and c; (d) L and K. The color bars represent the ranges of the interval of existence of the pseudo-equilibrium.

equilibrium $E^*_{S_0}$ becomes globally asymptotically stable. The changes in the length of the sliding segment for different values of L is shown in Fig. $7(c)$. Similarly, for $c = 0.5$ and other parameter values as in Table 1, the changes in the sliding mode due to the changes in the values of L is given in Fig. $7(d)$.

6 Prey vigilance and hysteresis effect

In the Filippov system (4), the dispersal of the prey from the unprotected zone to refuge protection is assumed to be instantaneous whenever the predator population crosses some critical threshold value. In reality, the movement of prey species between the two habitats involves some travel time. Apart from this, the reaction time of the prey plays a pivotal role in the switching delay. The slow or less vigilant prey will take more dispersion time than the fast or more vigilant

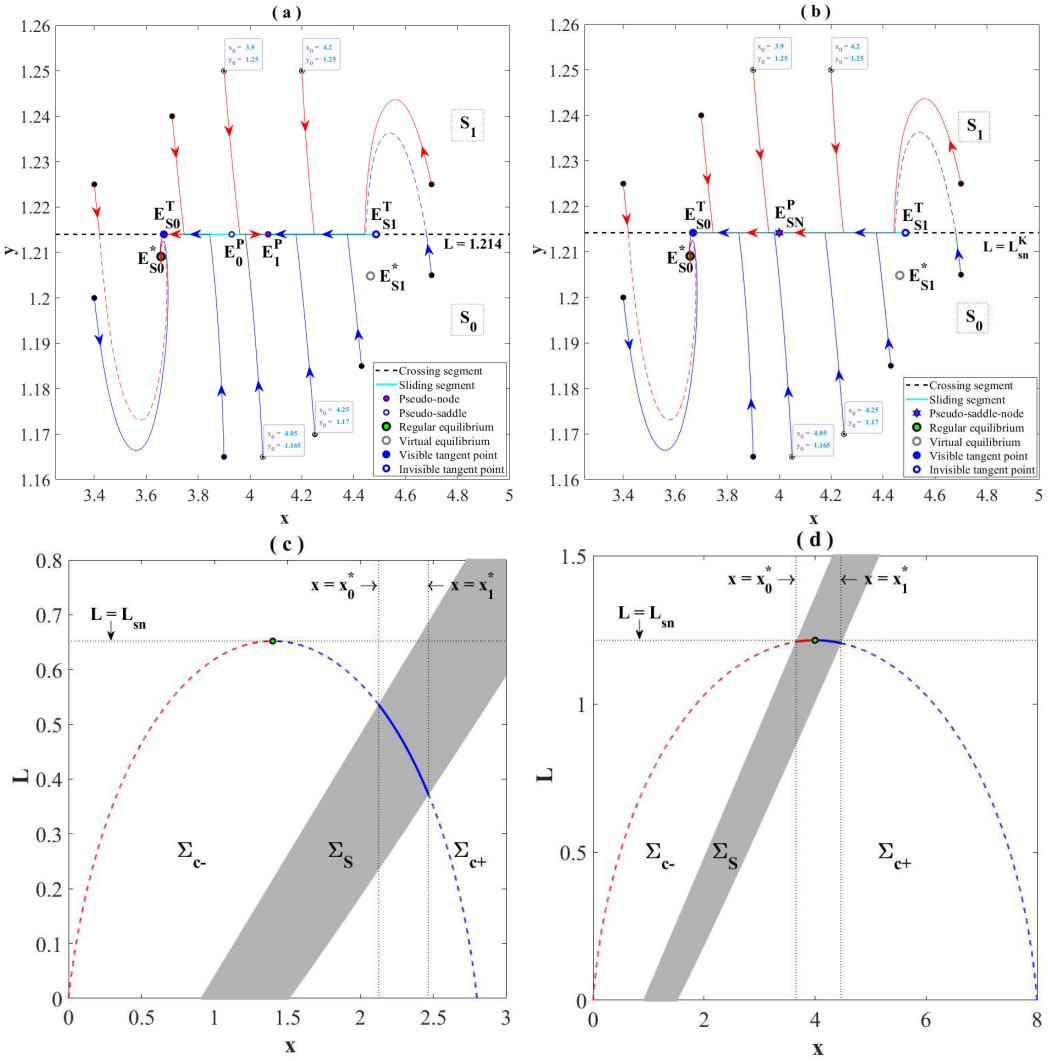

Fig. 6: A one parameter bifurcation plot of the system (4) with L as a bifurcation parameter, where $K = 8$ and other parameters values as in Table 1. (a) A pseudo-saddle (E_0^P) and a pseudo-node (E_1^P) exist on the sliding segment Σ_S for $L < L_{sn}^K$. (b) For $L = L_{sn}^K$, the generic pseudo-saddle-node E_{SN}^P exists on Σ_S. The evolution of the sliding modes (grey regions) with the changes in L for (c) all parameters values as in Table 1, where a pseudo-saddle-node bifurcation occurs on the crossing segment Σ_{c-} and for (d) for $K = 8$ and other parameters values as in Table 1, where a pseudo-saddle-node bifurcation occurs on the sliding segment Σ_S.

prey. Due to this delay in dispersion, the population threshold of the predators to enter the prey-refuge differs from the population threshold of predators to return to the unprotected zone. This delay in the dispersion of the prey leads to increased predation pressure. To monitor for such possibilities, we introduce the hysteresis effect on the system (4) which allows a period of over-exploitation of prey species without compromising its density. The modified Filippov system with hysteresis effect is given by

$$\dot{Z}(t) = F^0(Z) + U_H^h(Z), \tag{8}$$

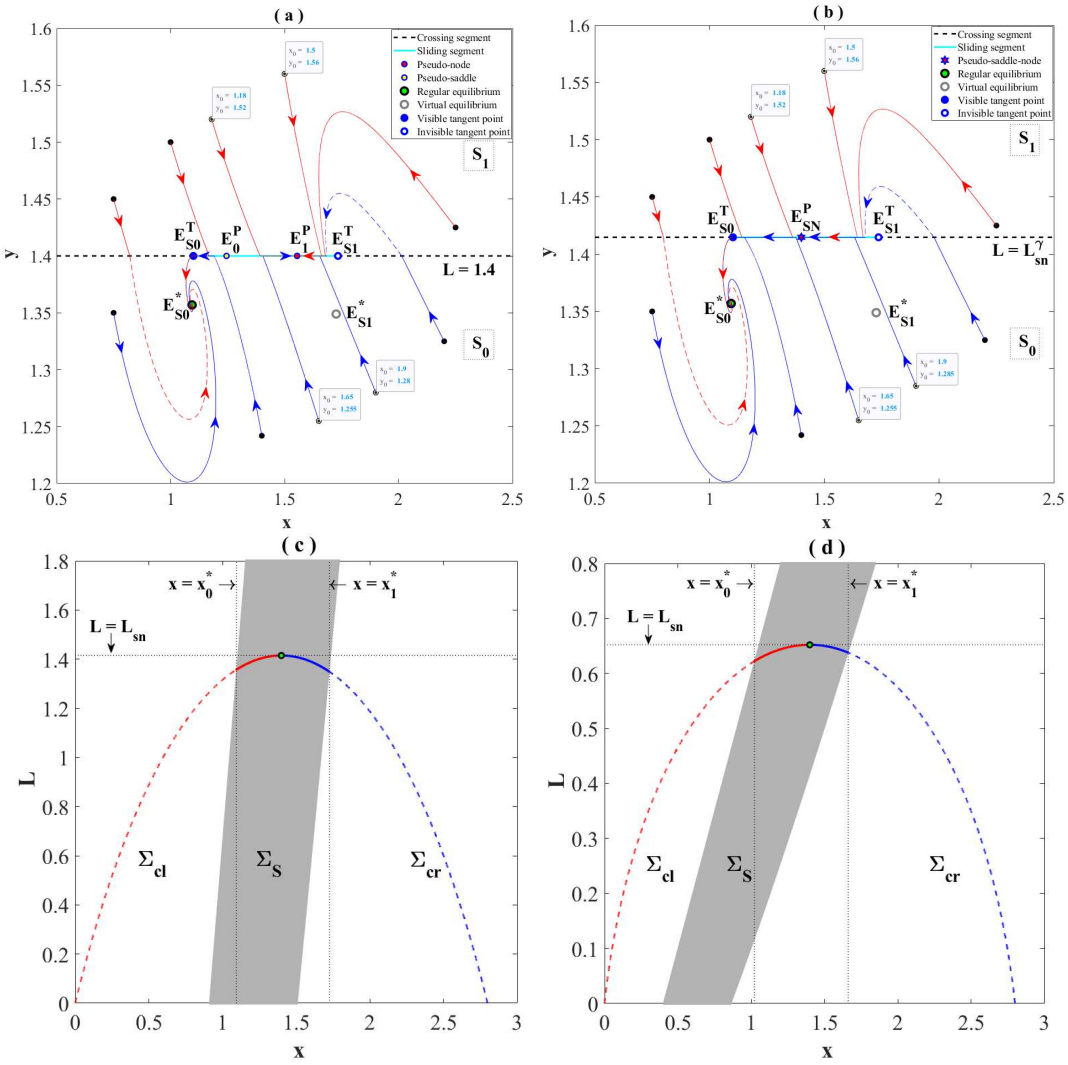

Fig. 7: Pseudo-saddle-node bifurcation of the system (4) for $\gamma = 0.015$ and L as a bifurcation parameter, other parameters values as in Table 1. (a) The existence of a pseudo-saddle (E_0^P) and a pseudo-node (E_1^P) on the sliding segment Σ_S for $L < L_{sn}^{\gamma}$. (b) For $L = L_{sn}^{\gamma}$, the generic pseudo-saddle-node E_{SN}^P exists on Σ_S. The evolution of the sliding modes (grey regions) with respect to the changes in L for (c) $\gamma = 0.015$ and for (d) $c = 0.5$, other parameters values as in Table 1.

with the control $U_H^h(Z)$ defined as

$$U_H^h(Z) = \begin{cases} (0,\,0)^T, & H(Z) < -\sigma \text{ or } H(Z) \le \sigma \text{ for } \dot{Z} > 0 \\ \left(\frac{\varepsilon c\alpha xy}{x+\beta}, -\frac{\varepsilon ec\alpha xy}{x+\beta}\right)^T, & H(Z) > \sigma \text{ or } H(Z) \ge -\sigma \text{ for } \dot{Z} < 0, \end{cases}$$

where $\sigma > 0$ is the hysteresis parameter. The hysteresis parameter σ, representing the level of vigilance of the prey, satisfies $0 < \sigma < |L - y_\varepsilon^*|$ so that the interior equilibria $E_{S_\varepsilon}^*$ are always virtual $(\varepsilon = 0, 1)$. The smaller values of σ represent hypervigilant prey, whereas the larger values of σ implies that the prey is less vigilant. For $\sigma > |L - y_\varepsilon^*|$, the collapse of prey stock becomes irreversible due to sustained predation pressure. The system (8) has the two switching lines

$$\Sigma_0 = \left\{Z \in \mathbf{R}_+^2 : H(Z) = -\sigma\right\} \text{ and } \Sigma_1 = \left\{Z \in \mathbf{R}_+^2 : H(Z) = \sigma\right\}.$$

The switching lines Σ_0 and Σ_1 generate the following regions in the state space,

$\Omega_0 = \{Z \in \mathbf{R}^2_+ : H(Z) < -\sigma\}$,

$\Omega_1 = \{Z \in \mathbf{R}^2_+ : H(Z) > \sigma\}$ and

$\Omega_2 = \{Z \in \mathbf{R}^2_+ : -\sigma \leq H(Z) \leq \sigma\}$.

The trajectories that start from Ω_0 and evolve towards Ω_1 has the threshold Σ_1, whereas the trajectories that start from Ω_1 and evolve towards Ω_0 has the threshold Σ_0 (cf. Fig. 8). Let the vector $H_Z(Z)$, normal to Σ_1 and Σ_2, is oriented in the direction from Ω_0 to Ω_1. The curves $V_{S_\varepsilon}(Z) = L_{F^\varepsilon}H(Z) = 0$ $(\varepsilon = 0, 1)$, subdivide the state phase into the following four regions:

$R_1 = \{Z \in \mathbf{R}^2_+ : L_{F^0}H(Z) > 0\}$,

$R_2 = \{Z \in \mathbf{R}^2_+ : L_{F^0}H(Z) < 0\}$,

$R_3 = \{Z \in \mathbf{R}^2_+ : L_{F^1}H(Z) > 0\}$ and

$R_4 = \{Z \in \mathbf{R}^2_+ : L_{F^1}H(Z) < 0\}$.

We use the geometrical approach proposed by Boukal and Krivan [9] to prove the existence of a trapping region in the state space where the trajectories of the system (8) enter with a transversal motion.

Lemma 6.1 *If $\sigma < |L - y^*_\varepsilon|$ $(\varepsilon = 0, 1)$ and $\Omega = \Omega_2 \bigcap R_1 \bigcap R_4$ is of non-zero measure, then Ω is a trapping region.*

Proof Choosing $0 < \sigma < |x^*_\varepsilon - x_0|$, from Fig. 8 we see that both the interior equilibria $E^*_{S_\varepsilon}$ $(\varepsilon = 0, 1)$ become virtual. To determine the direction of the vector field on the switching lines Σ_0 and Σ_1, we examine the signs of $L_{F^0}H(Z)$ and $L_{F^1}H(Z)$.

Let A and D be the points of intersection of the curve $V_{S_0}(Z) = 0$ with the switching lines Σ_0 and Σ_1 respectively (cf. Fig. 8), where $A = \left(\frac{\gamma(L-\sigma)+\delta}{ec},\, L - \sigma\right)$, $D = (x_{L-\sigma},\, L - \sigma)$ and

$$x_{L-\sigma} = \frac{-\{ec(\beta-\alpha) - \gamma(L-\sigma) - \delta\} + \sqrt{\{ec(\beta-\alpha) - \gamma(L-\sigma) - \delta\}^2 + 4ec\beta\{\gamma(L-\sigma) + \delta\}}}{2ec}.$$

On the switching line Σ_0, $L_{F^0}H(Z) > 0$ implies $y > \frac{ecx-\delta}{\gamma}$ and so, the trajectories starting from Ω_0 and moves below the line segment AH_2, enter the region Ω (cf. Fig. $8(a)$). The points that satisfy $L_{F^0}H(Z) > 0$ lie on the right of the curve $V_{S_0}(Z) = 0$ in the region $R_1 \bigcap (R_3 \bigcup R_4)$ (cf. Fig. $8(c)$).

Let B and C be the points of intersection of the curve $V_{S_1}(Z) = 0$ with the switching lines Σ_0 and Σ_1 respectively, where $B = \left(\frac{\gamma(L+\sigma)+\delta}{ec},\, L + \sigma\right)$, $C = (x_{L+\sigma},\, L + \sigma)$ and

$$x_{L+\sigma} = \frac{-\{ec(\beta-\alpha) - \gamma(L+\sigma) - \delta\} + \sqrt{\{ec(\beta-\alpha) - \gamma(L+\sigma) - \delta\}^2 + 4ec\beta\{\gamma(L+\sigma) + \delta\}}}{2ec}.$$

On the switching line Σ_1, $L_{F^1}H(Z) < 0$ implies $y < \frac{ecx(x+\beta-\alpha)-\delta(x+\beta)}{\gamma(x+\beta)}$ and so, the trajectories starting from Ω_1 and evolve above the line segment CH_4, enter the region Ω (cf. Fig. $8(b)$). The points that satisfy $L_{F^1}H(Z) < 0$ lie left of the curve $V_{S_1}(Z) = 0$ in the region $R_4 \bigcap (R_1 \bigcup R_2)$ (cf. Fig. $8(c)$).

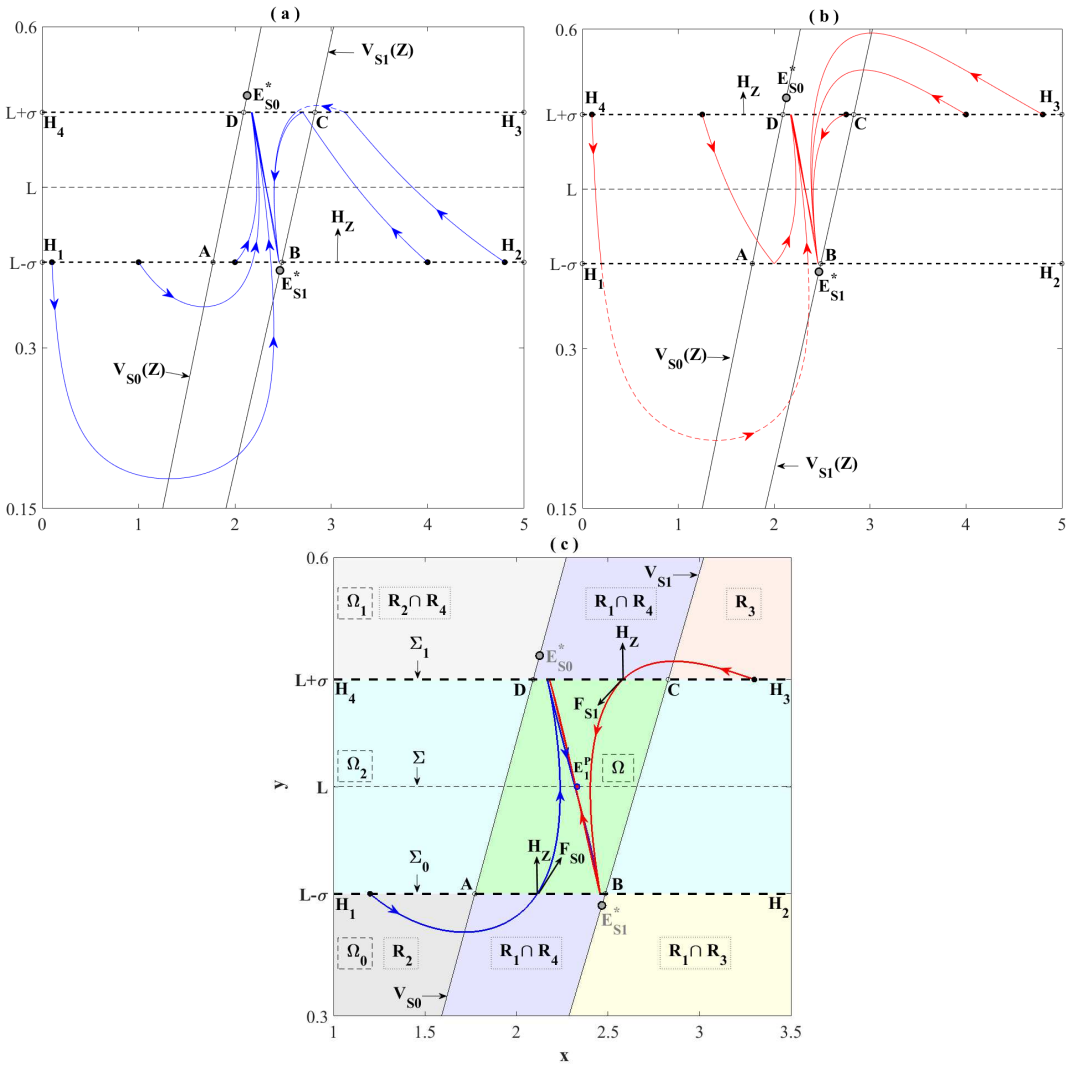

Fig. 8: A representation of intermittent dispersal with hysteresis in the region Ω bounded by lines Σ_0 and Σ_1.

The trajectories that enter into the region Ω_2 with a transversal motion and satisfies $L_{F^0}H(Z) > 0, L_{F^1}H(Z) < 0$, stays in $R_1 \bigcap R_4$. From Fig. $8(a)$ it is seen that the trajectories of (8) with an initial points below Σ_0 intersect the switching line Σ_1 at a point on the line segment CD and remains within $\Omega = \Omega_2 \bigcap R_1 \bigcap R_4$. The trajectories with an initial point above Σ_1 intersect the switching line Σ_0 at some point on the line segment AB and stays in Ω thenceforth. This implies that the trajectories with a transversal motion enter Ω of non-zero measure and stays there forever. Therefore, the region Ω is a trapping region and so, a hysteresis loop around the predator population threshold L stabilizes the system (8) through low amplitude oscillations in the bounded region Ω.

From Fig. $8(c)$ we observe that during the period of prey-refuge, the trajectories of the system (8) stay in the region Ω_2 and are directed towards the switching line Σ_1. Therefore, the time taken by the trajectories of the system (8) to reach the switching line Σ_1 after hitting the switching line Σ_0 can be regarded as the refuge time period of the prey. At this time, the predation pressure on the prey is quite low owing to the prey refuge protection. Similarly, the time taken

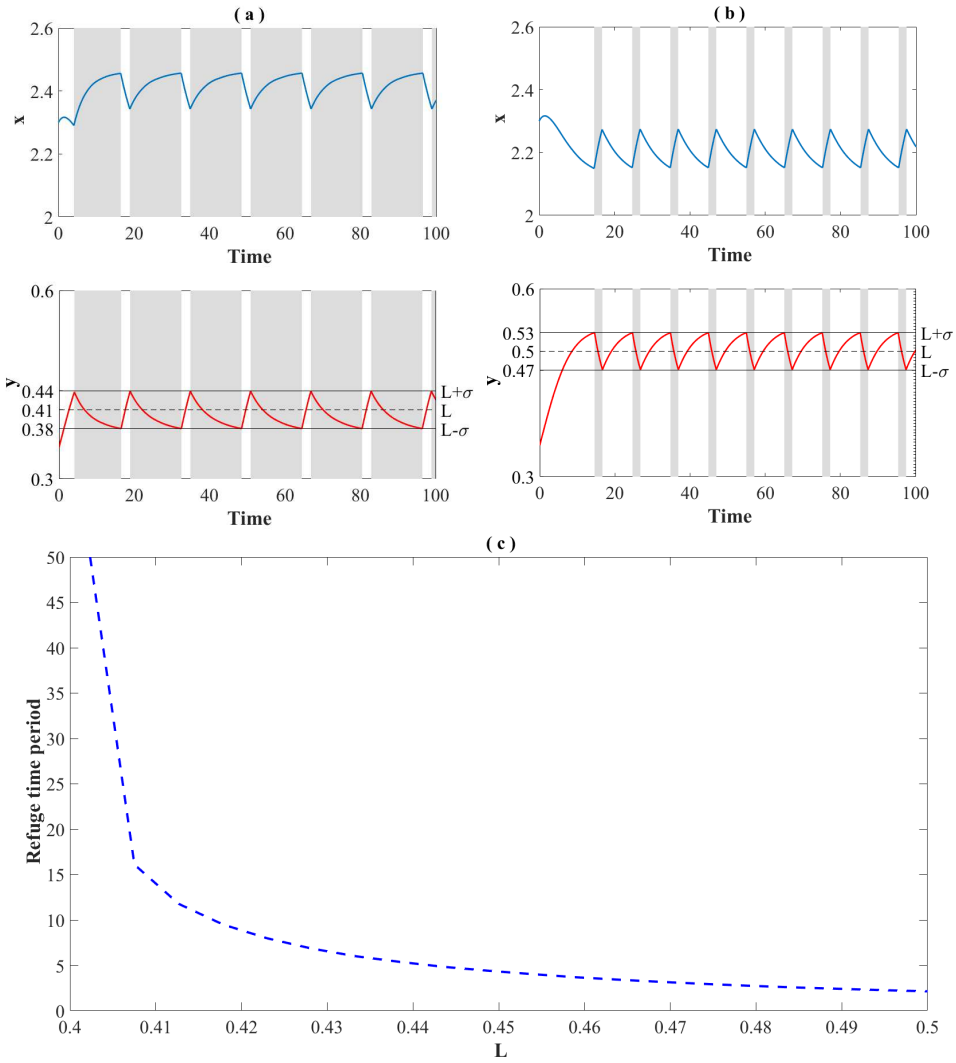

Fig. 9: The time evolution of the population when the prey species is (a) apprehensive $(L = 0.41)$ or (b) bold $(L = 0.5)$, but with equally vigilant $(\sigma = 0.03)$. (c) For $\sigma = 0.03$, the changes in the refuge stay time period with L as an active parameter. The shaded regions indicate the time spent by the prey in refuge.

by the trajectories of the system (8) to reach the switching line Σ_0 after hitting Σ_1 refers to the non-refuge period. The non-refuge period refers to the time of over-exploitation of the prey by the predators. To determine the changes in the refuge time period owing to the changes in the threshold population density of the predators, we vary L subject to the condition $y_1^* + \sigma < L < y_0^* - \sigma$ while all other parameter values remain unaltered. From Figs. $9(a)$ and $9(b)$ it follows that with an increase of L, there is a drop in the time period in the refuge. Therefore, with an increase in the predator population density, the more apprehensive prey is most likely to avail refuge protection, while the population of the bold prey will decrease due to the increased predation pressure (cf. Fig. $9(c)$).

By increasing the parameter σ in the domain $0 < \sigma < |L - y_\varepsilon^*|$ and keeping all other parameters of the system fixed, from Figs. $10(a)$ and $10(b)$ we observe that the prey prefers to take refuge protection for a longer time period. This

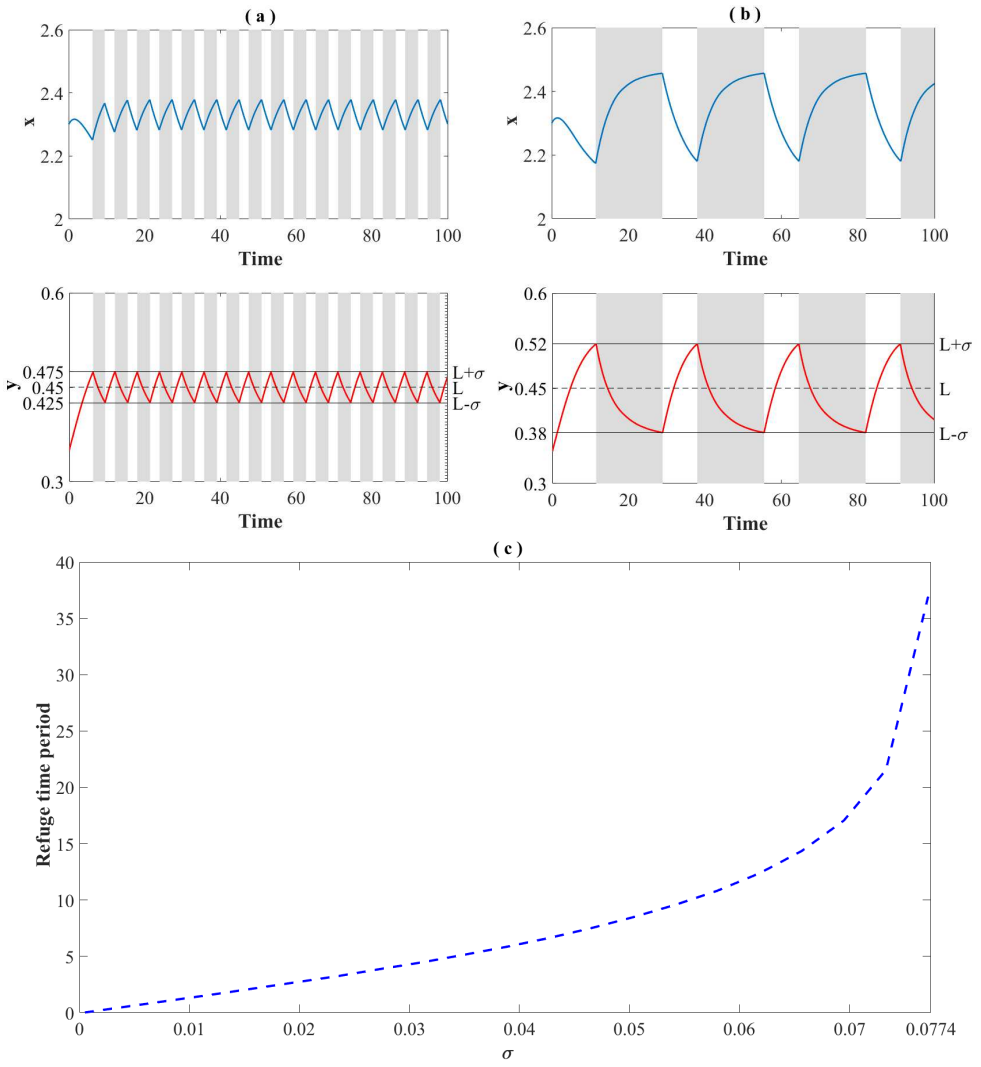

Fig. 10: The time evolution of the population when the prey species is (a) is hypervigilant $(\sigma = 0.025)$ or (b) less vigilant $(\sigma = 0.07)$, but with the fixed level of apprehension $(L = 0.45)$. (c) For $L = 0.45$, the changes in the refuge stay time period with σ as an active parameter. The shaded regions indicate the time spent by the prey in refuge.

implies that the relatively less vigilant prey will stay in refuge protection for a longer period even when the predator population density drops significantly and will stay in the open habitat for a longer period even when the predator population becomes high. Frequent switching of habitat of the prey from the refuge to the open habitat happens when the hysteresis parameter value is low. In this case, the predator population density fluctuates from $L-\sigma$ to $L+\sigma$. Therefore, hypervigilant prey species are most likely to move to and fro from the open habitat to the refuge depending on the changes in the population density of the predators.

To study the combined effect of L and σ on the refuge time period, we divide the $L\sigma$-parameter plane into the following four regions:

Region-$I = \{(L,\sigma) \in \mathbf{R}^2_+ : 0 < L+\sigma \leq y^*_0,\ L-\sigma \geq y^*_1\}$,

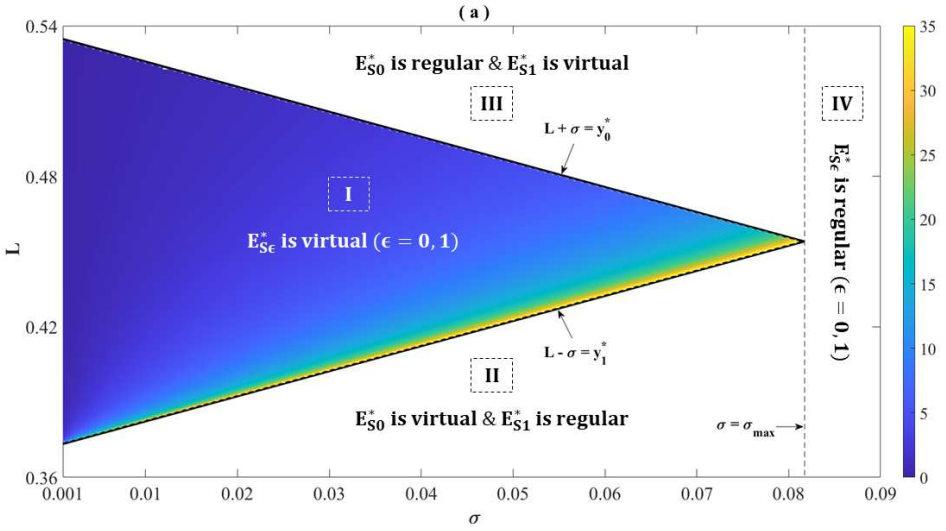

Fig. 11: The time spent in refuge as a function of prey apprehension (L) and vigilance (σ). The colour bar represents the refuge time period.

Region-$II = \{(L,\sigma) \in \mathbf{R}^2_+ : 0 < L+\sigma \leq y_0^*,\ 0 < L-\sigma < y_1^*\}$,

Region-$III = \{(L,\sigma) \in \mathbf{R}^2_+ : L+\sigma > y_0^*,\ L-\sigma \geq y_1^*\}$ and

Region-$IV = \{(L,\sigma) \in \mathbf{R}^2_+ : L+\sigma > y_0^*,\ 0 < L-\sigma < y_1^*\}$.

The regions I, II, III and IV in the $\sigma - L$ parameter plane (cf. Fig. 11) represent the region of intermittent refuge protection, continuous refuge protection, no refuge protection, and compromised refuge respectively. We know that the switching mode is possible only in the region I and the predator population fluctuates in between $L-\sigma$ to $L+\sigma$. At a threshold population density L of the predators, the maximum value of the hysteresis parameter is $\sigma_L = \min\{L-y_1^*, y_0^*-L\}$. When the threshold predator population value is $\frac{1}{2}(y_0^*+y_1^*)$, the hysteresis parameter reaches its global maximum $\sigma_{\max} = \frac{1}{2}(y_0^*-y_1^*)$; and consequently, the refuge time period becomes maximum. In the region II, the predator population is greater than $L+\sigma$, whereas in the region III, the predator population is less than $L-\sigma$. In the region IV, we have $\sigma > \sigma_{\max}$ and so the least vigilant prey will continue to stay in the same habitat irrespective of the changes in the predator population density. In this case, the prey will be deprived of foraging or mating opportunities due to their continuous stay at the refuge or the prey population gets severely compromised due to their continuous stay at the open habitat. It is observed that prey can be hypervigilant as well as bold (or apprehensive). In either case, the prey frequently switches their habitat due to the changes in the predator population. A bold and less vigilant prey continues to stay in the open habitat by compromising their stock (region III), whereas a more apprehensive and less vigilant prey prefer staying at the refuge by compromising their foraging and mating opportunities in the open habitat (region II). We also observed that the more apprehensive prey (in the region I) prefers to stay for a longer time at the refuge even if they are hypervigilant.

7 Discussion

In this paper, we have studied a non-smooth system with density-dependent intermittent refuge protection of the prey by employing Filippov's convex method and Utkin's equivalent control method. The qualitative analyses for the subsystems of the Filippov system were carried out, confirming the non-existence of periodic solutions of the subsystems and giving the threshold conditions for the existence of transcritical bifurcations. We obtained the conditions for the existence of the regular and virtual equilibrium, boundary equilibrium, tangent points and pseudo-equilibrium of the Filippov system. We verified the existence of a pair of pseudo-equilibria when the level of apprehension of the prey is less than some threshold value. Under this level of prey apprehension, we have shown that one of the pseudo-equilibria is a saddle point and the other one is a stable node. We investigated regular or virtual equilibrium bifurcation, boundary-node bifurcation and pseudo-saddle-node bifurcation. We studied the effect of hysteresis in the Filippov system by introducing switching delay arising due to different behavioural traits of the prey species. We identified the evolution of stable limit cycles around the threshold population density of the predators in some bounded region in the phase space due to the delay in the switching of habitat.

From numerical simulations, we observed that a highly apprehensive prey has a longer refuge stay time compared to a bold prey. We also observed that a hypervigilant prey frequently switches their habitat compared to their less vigilant counterpart, whereas a less vigilant prey overstays either in the refuge or in the open habitat depending upon the population density of the predators. Irrespective of the level of apprehension of the prey, the hypervigilant prey frequently switches their habitat due to the changes in the predator population, decoupling prey vigilance and apprehension. We also observed that a bold and less vigilant prey continues to stay in the open habitat by compromising their stock, whereas a more apprehensive and less vigilant prey prefers staying at the refuge by compromising their foraging and mating opportunities in the open habitat.

Acknowledgment

JB is supported by the grants from Science and Engineering Research Board (SERB), Govt. of India (File No. TAR/2018/000283).

Funding SERB, India (File No. TAR/2018/000283).

Declarations

Conflict of Interest The authors declare that they have no conflict of interest.

Availability of data and material Not applicable.

Code availability Not applicable.

Ethics approval Not applicable.

References

1. Amo, L., López, P., Martín, J.: Refuge use: a conflict between avoiding predation and losing mass in lizards. Physiology & Behavior **90**(2-3), 334–343 (2007)
2. Beauchamp, G.: What can vigilance tell us about fear? Animal Sentience **2**(15), 1 (2017)
3. Beauchamp, G.: External body temperature and vigilance to a lesser extent track variation in predation risk in domestic fowls. BMC Zoology **4**(1), 1–8 (2019)
4. Belgrad, B.A., Griffen, B.D.: Predator–prey interactions mediated by prey personality and predator hunting mode. Proceedings of the Royal Society B: Biological Sciences **283**(1828), 20160408 (2016)
5. Berezovskaya, F.S., Song, B., Castillo-Chavez, C.: Role of prey dispersal and refuges on predator-prey dynamics. SIAM Journal on Applied Mathematics **70**(6), 1821–1839 (2010)
6. Bhattacharyya, J., Roelke, D.L., Pal, S., Banerjee, S.: Sliding mode dynamics on a prey–predator system with intermittent harvesting policy. Nonlinear Dynamics **98**(2), 1299–1314 (2019)
7. Bhattacharyya, J., Roelke, D.L., Walton, J.R., Banerjee, S.: Using *yy* supermales to destabilize invasive fish populations. Theoretical Population Biology **134**, 1–14 (2020)
8. Blake, C.A., Andersson, M.L., Hulthén, K., Nilsson, P.A., Brönmark, C.: Conspecific boldness and predator species determine predation-risk consequences of prey personality. Behavioral Ecology and Sociobiology **72**(8), 133 (2018)
9. Boukal, D.S., et al.: Lyapunov functions for lotka–volterra predator–prey models with optimal foraging behavior. Journal of Mathematical Biology **39**(6), 493–517 (1999)
10. Brown, G.E., Rive, A.C., Ferrari, M.C., Chivers, D.P.: The dynamic nature of antipredator behavior: prey fish integrate threat-sensitive antipredator responses within background levels of predation risk. Behavioral Ecology and Sociobiology **61**(1), 9–16 (2006)
11. Carthey, A.J., Bucknall, M.P., Wierucka, K., Banks, P.B.: Novel predators emit novel cues: a mechanism for prey naivety towards alien predators. Scientific reports **7**(1), 1–9 (2017)
12. Chattopadhyay, J., Bairagi, N., Sarkar, R.: A predator-prey model with some cover on prey species. Nonlinear Phenomena in Complex Systems-Minsk **3**(4), 407–420 (2000)
13. Chen, L., Chen, F., Chen, L.: Qualitative analysis of a predator–prey model with holling type ii functional response incorporating a constant prey refuge. Nonlinear Analysis: Real World Applications **11**(1), 246–252 (2010)
14. Chittka, L., Skorupski, P., Raine, N.E.: Speed–accuracy tradeoffs in animal decision making. Trends in ecology & evolution **24**(7), 400–407 (2009)
15. Choh, Y., Ignacio, M., Sabelis, M.W., Janssen, A.: Predator-prey role reversals, juvenile experience and adult antipredator behaviour. Scientific Reports **2**, 728 (2012)
16. Cooper Jr, W.E., Perez-Mellado, V.: Historical influence of predation pressure on escape by podarcis lizards in the balearic islands. Biological Journal of the Linnean Society **107**(2), 254–268 (2012)
17. Donelan, S.C., Grabowski, J.H., Trussell, G.C.: Refuge quality impacts the strength of nonconsumptive effects on prey. Ecology **98**(2), 403–411 (2017)

18. Dowling, L.M., Godin, J.G.J.: Refuge use in a killifish: influence of body size and nutritional state. Canadian Journal of Zoology **80**(4), 782–788 (2002)
19. Drakunov, S.V., Utkin, V.I.: Sliding mode control in dynamic systems. International Journal of Control **55**(4), 1029–1037 (1992)
20. Fardell, L.L., Pavey, C.R., Dickman, C.R.: Fear and stressing in predator–prey ecology: considering the twin stressors of predators and people on mammals. PeerJ **8**, e9104 (2020)
21. Feyten, L.E., Brown, G.E.: Ecological uncertainty influences vigilance as a marker of fear. Animal Sentience **2**(15), 7 (2018)
22. Filippov, A.F.: Differential equations with discontinuous righthand sides: control systems, vol. 18. Springer Science & Business Media (2013)
23. Hauzy, C., Gauduchon, M., Hulot, F.D., Loreau, M.: Density-dependent dispersal and relative dispersal affect the stability of predator–prey metacommunities. Journal of theoretical biology **266**(3), 458–469 (2010)
24. Jana, D., Ray, S.: Impact of physical and behavioral prey refuge on the stability and bifurcation of gause type filippov prey-predator system. Modeling Earth Systems and Environment **2**(1), 24 (2016)
25. Ji, L., Wu, C.: Qualitative analysis of a predator–prey model with constant-rate prey harvesting incorporating a constant prey refuge. Nonlinear Analysis: Real World Applications **11**(4), 2285–2295 (2010)
26. Kar, T.K.: Modelling and analysis of a harvested prey–predator system incorporating a prey refuge. Journal of Computational and Applied Mathematics **185**(1), 19–33 (2006)
27. Kavaliers, M., Choleris, E.: Antipredator responses and defensive behavior: ecological and ethological approaches for the neurosciences. Neuroscience & Biobehavioral Reviews **25**(7-8), 577–586 (2001)
28. Křivan, V.: Behavioral refuges and predator–prey coexistence. Journal of Theoretical Biology **339**, 112–121 (2013)
29. Manarul Haque, M., Sarwardi, S.: Dynamics of a harvested prey–predator model with prey refuge dependent on both species. International Journal of Bifurcation and Chaos **28**(12), 1830040 (2018)
30. Martin, R.A., Hammerschlag, N.: Marine predator–prey contests: ambush and speed versus vigilance and agility. Marine Biology Research **8**(1), 90–94 (2012)
31. Mirza, R.S., Ferrari, M.C., Kiesecker, J.M., Chivers, D.P.: Responses of american toad tadpoles to predation cues: behavioural response thresholds, threat-sensitivity and acquired predation recognition. Behaviour **143**(7), 877–889 (2006)
32. Perko, L.: Differential equations and dynamical systems, vol. 7. Springer Science & Business Media (2013)
33. Reaney, L.T.: Foraging and mating opportunities influence refuge use in the fiddler crab, uca mjoebergi. Animal Behaviour **73**(4), 711–716 (2007)
34. Ruxton, G.: Short term refuge use and stability of predator-prey models. Theoretical Population Biology **47**(1), 1–17 (1995)
35. Sih, A.: Prey refuges and predator-prey stability. Theoretical Population Biology **31**(1), 1–12 (1987)
36. Sih, A., Cote, J., Evans, M., Fogarty, S., Pruitt, J.: Ecological implications of behavioural syndromes. Ecology letters **15**(3), 278–289 (2012)
37. Tang, G., Tang, S., Cheke, R.A.: Global analysis of a holling type ii predator–prey model with a constant prey refuge. Nonlinear Dynamics **76**(1), 635–647 (2014)
38. Utkin, V.I.: Sliding modes in control and optimization. Springer Science & Business Media (2013)
39. Welp, T., Rushen, J., Kramer, D., Festa-Bianchet, M., De Passille, A.: Vigilance as a measure of fear in dairy cattle. Applied Animal Behaviour Science **87**(1-2), 1–13 (2004)
40. Zhou, Y., Sun, W., Song, Y., Zheng, Z., Lu, J., Chen, S.: Hopf bifurcation analysis of a predator–prey model with holling-ii type functional response and a prey refuge. Nonlinear Dynamics **97**(2), 1439–1450 (2019)

Figures

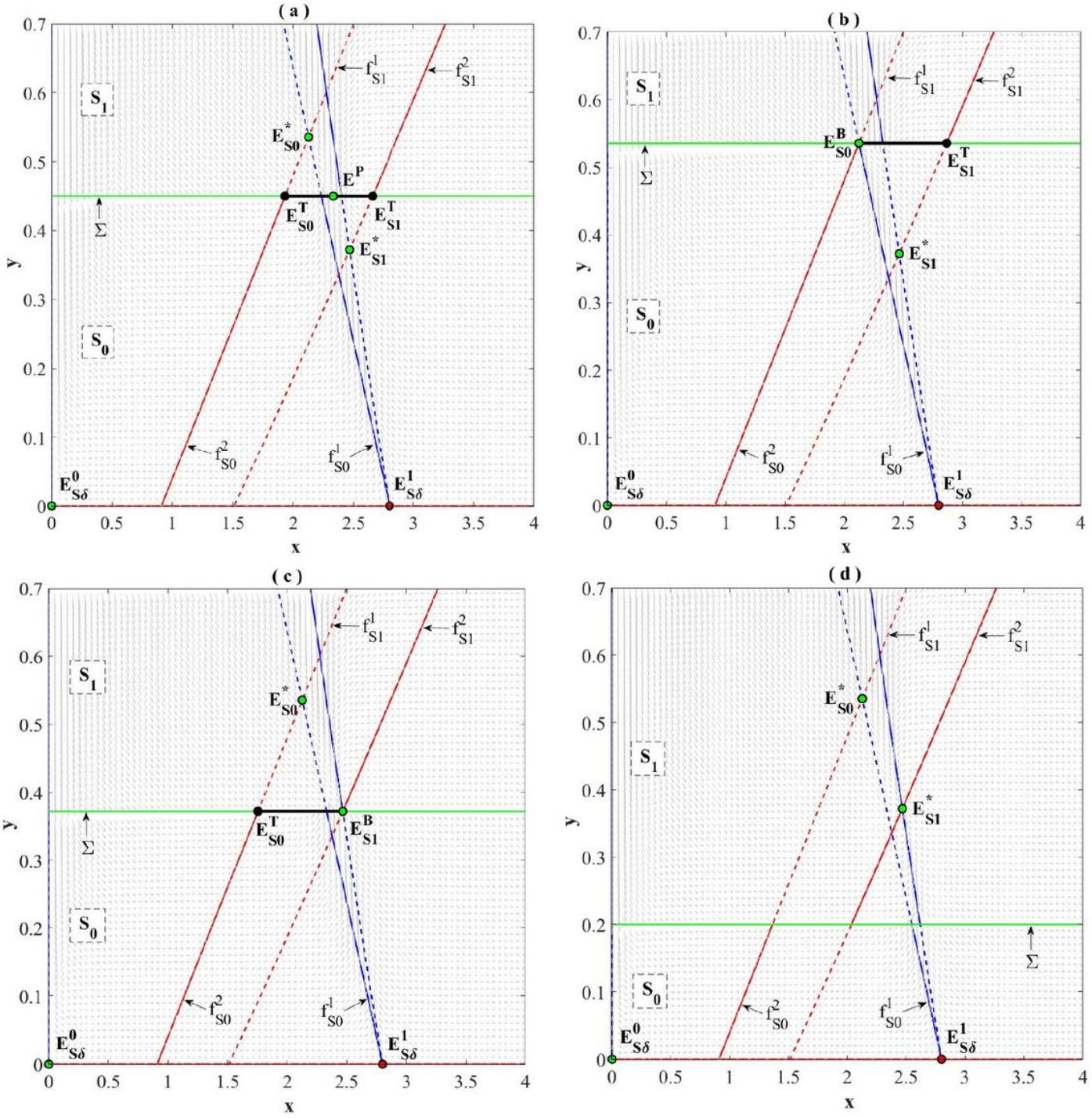

Figure 1

Please see the Manuscript PDF file for the complete figure caption

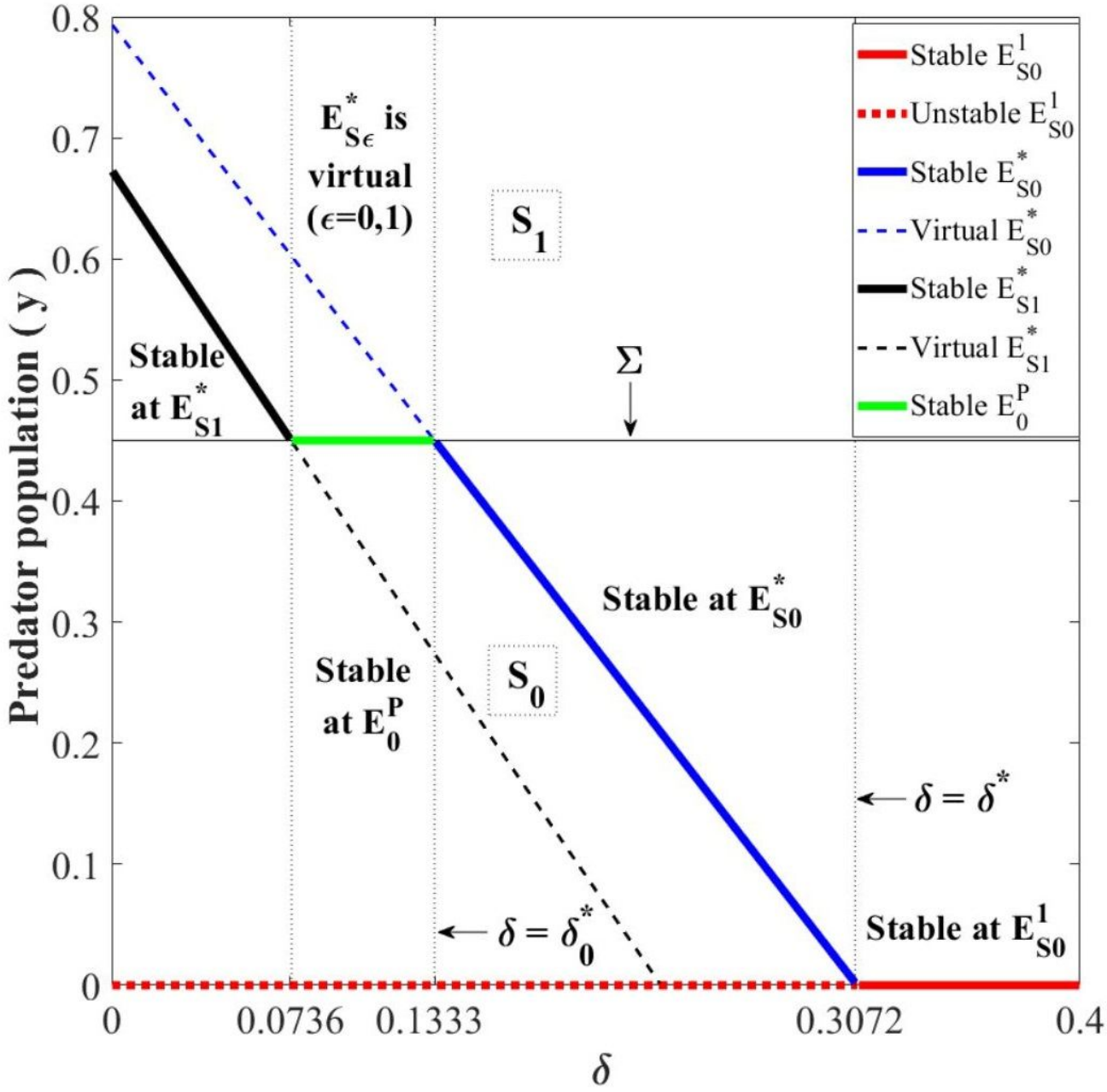

Figure 2

Please see the Manuscript PDF file for the complete figure caption

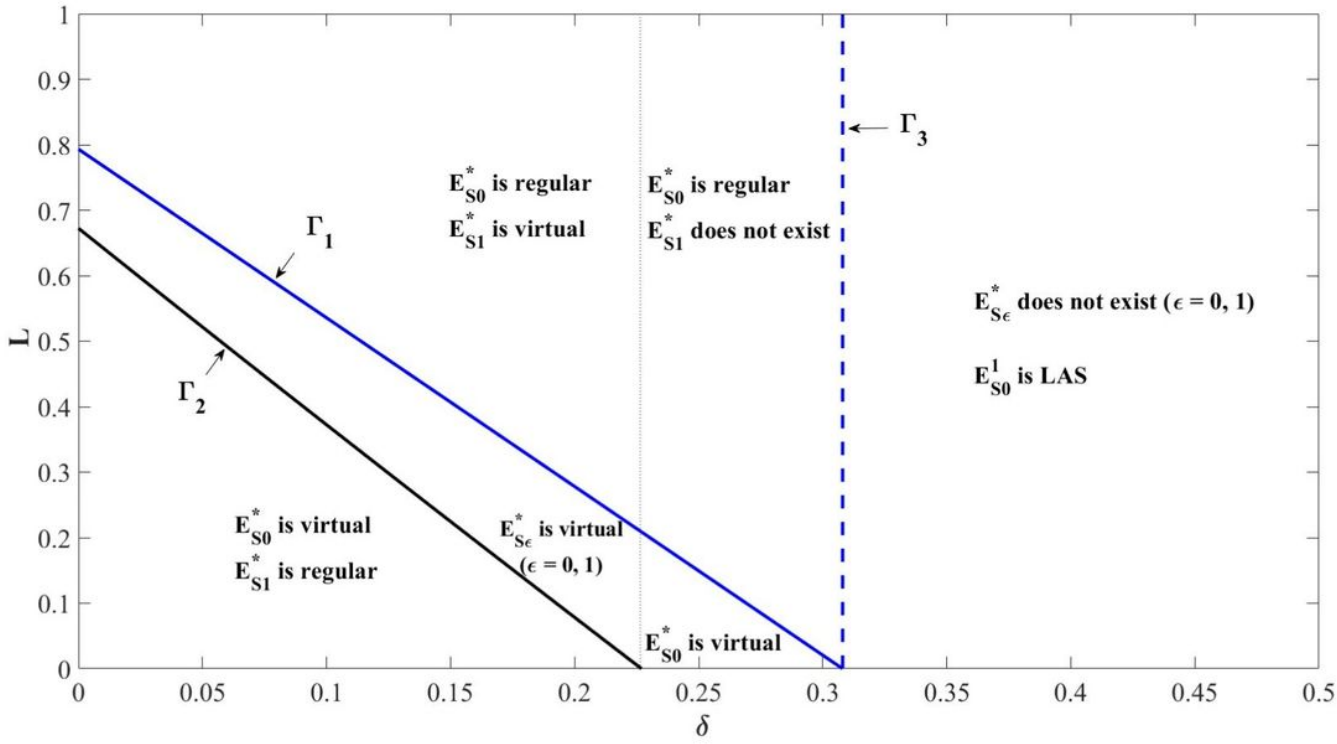

Figure 3

Please see the Manuscript PDF file for the complete figure caption

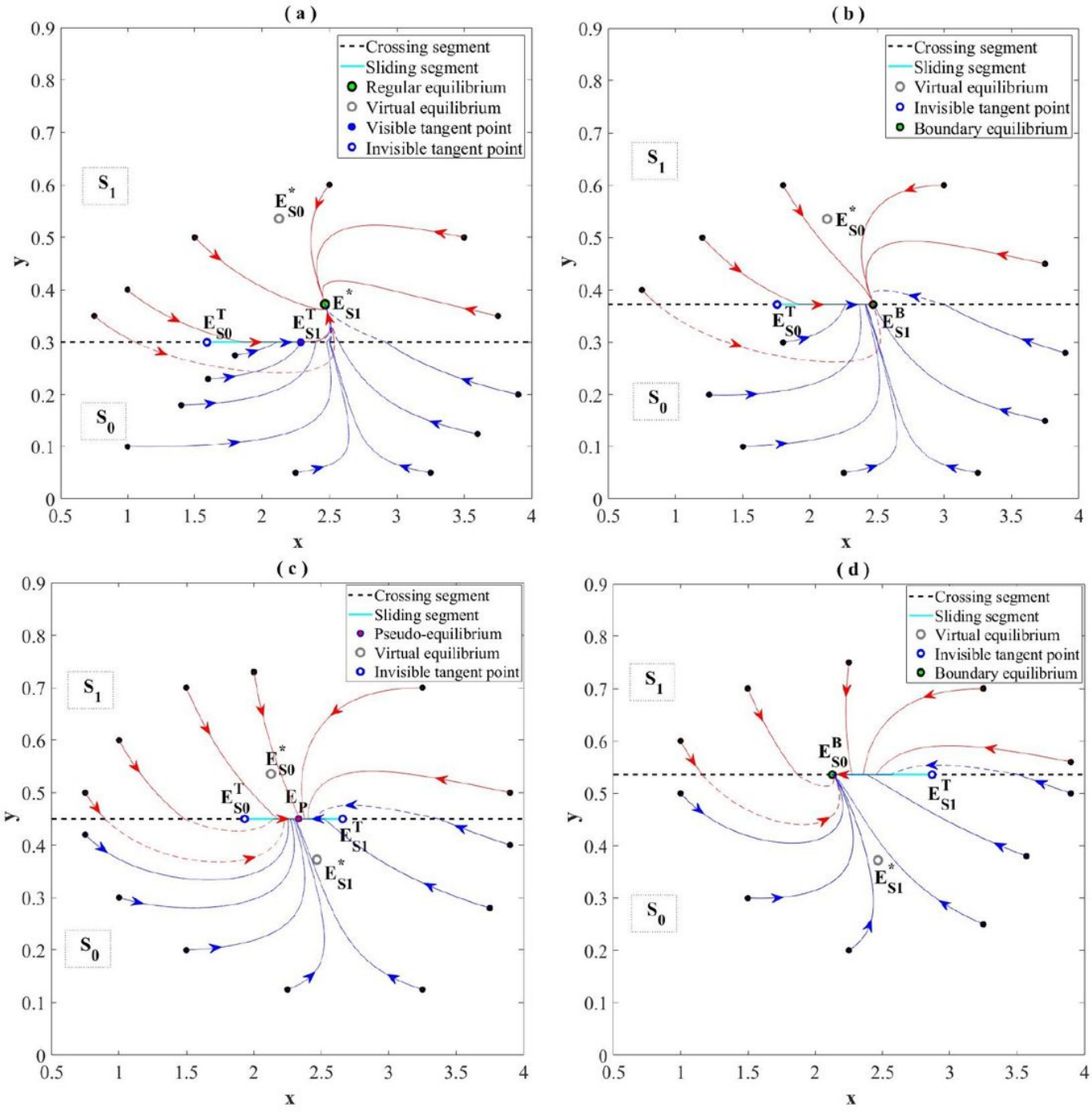

Figure 4

Please see the Manuscript PDF file for the complete figure caption

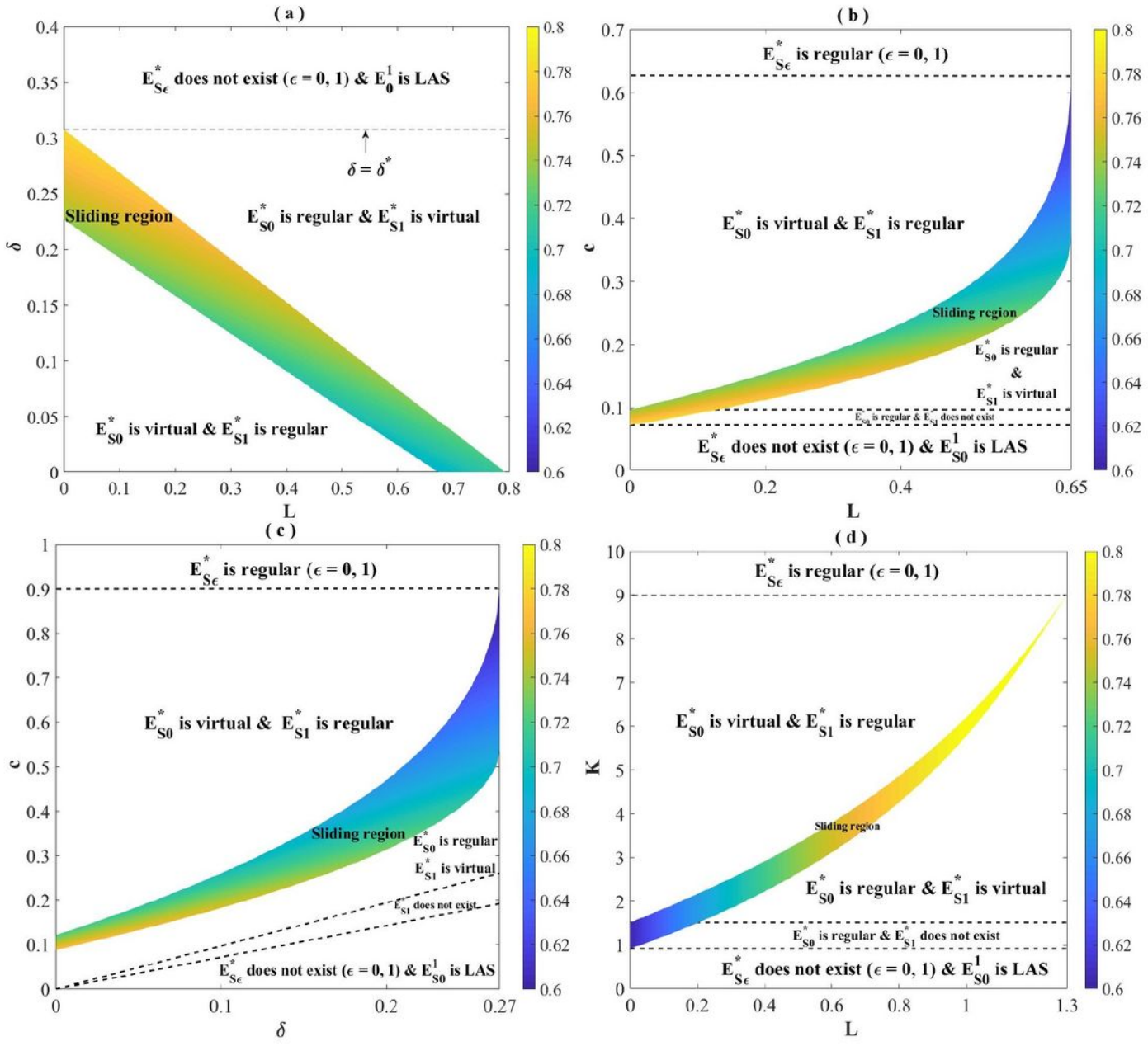

Figure 5

Please see the Manuscript PDF file for the complete figure caption

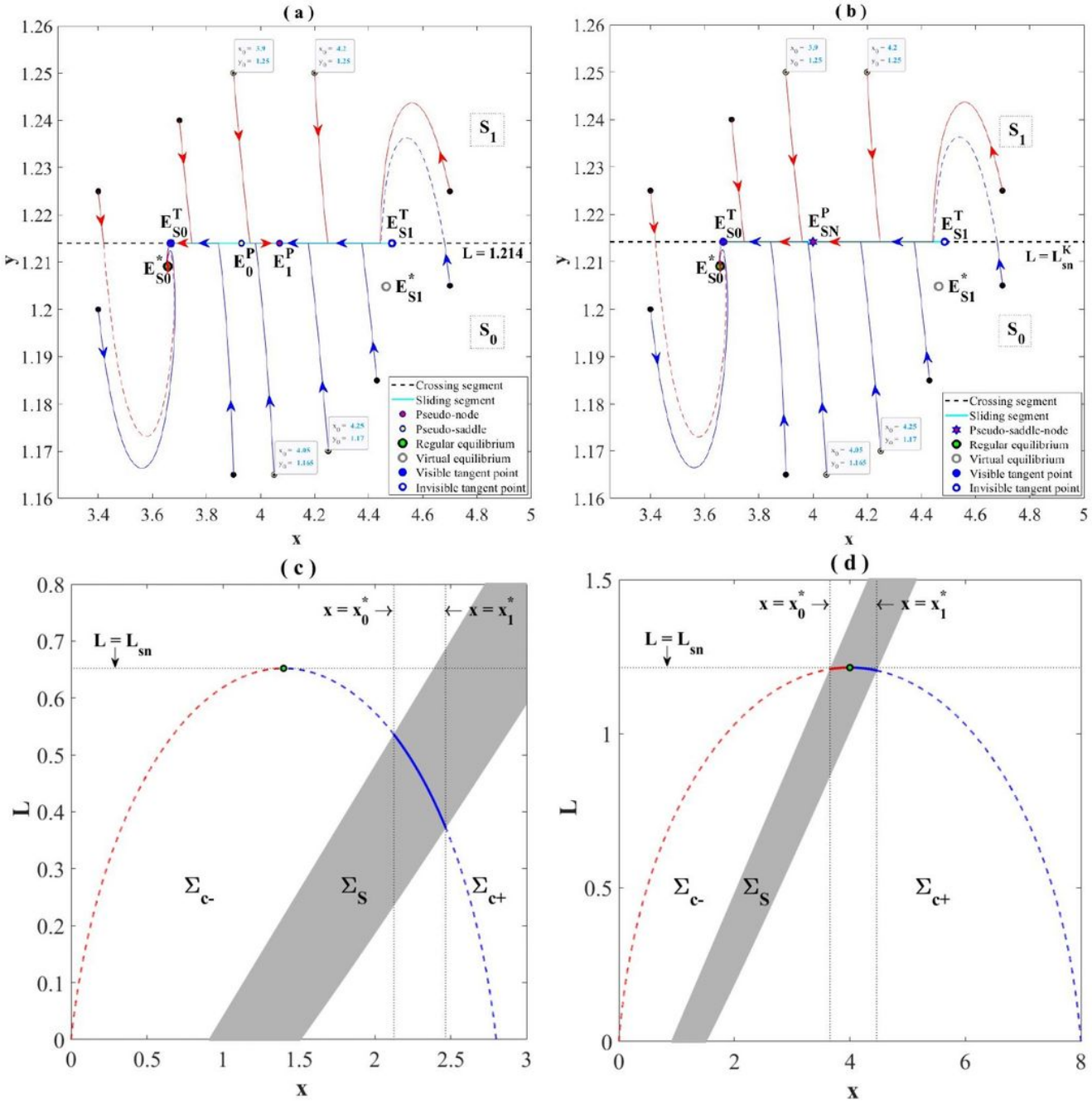

Figure 6

Please see the Manuscript PDF file for the complete figure caption

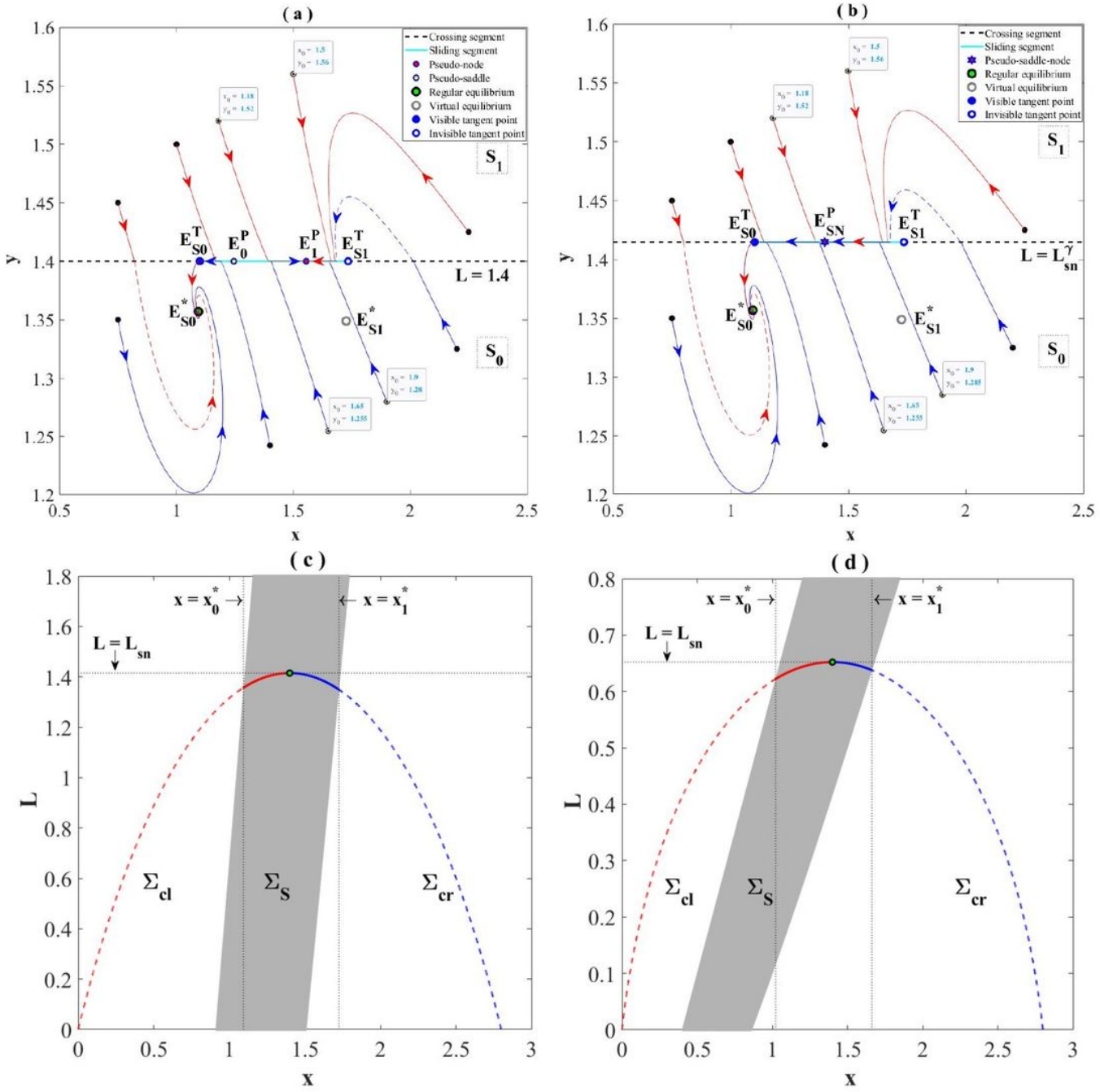

Figure 7

Please see the Manuscript PDF file for the complete figure caption

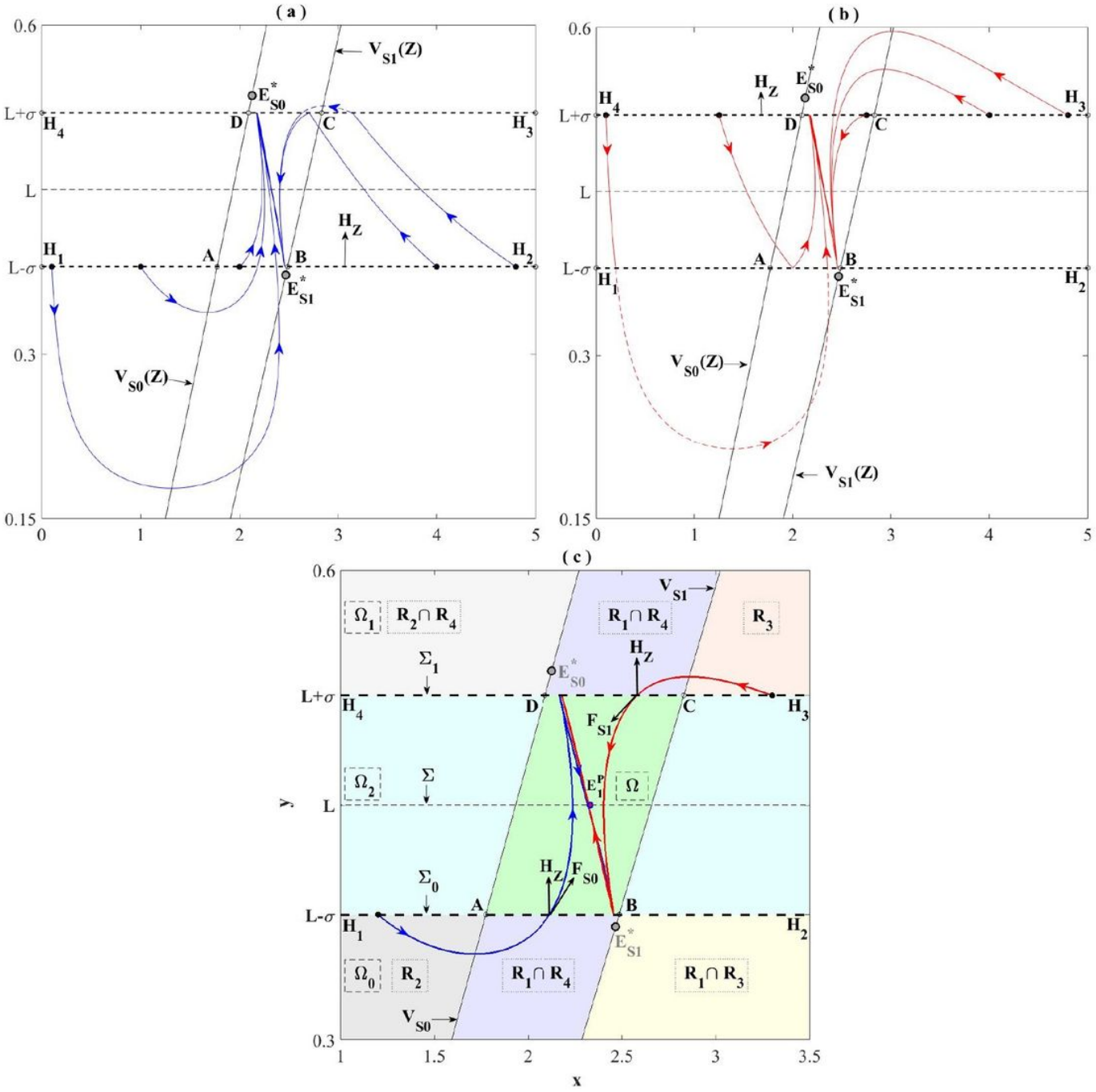

Figure 8

Please see the Manuscript PDF file for the complete figure caption

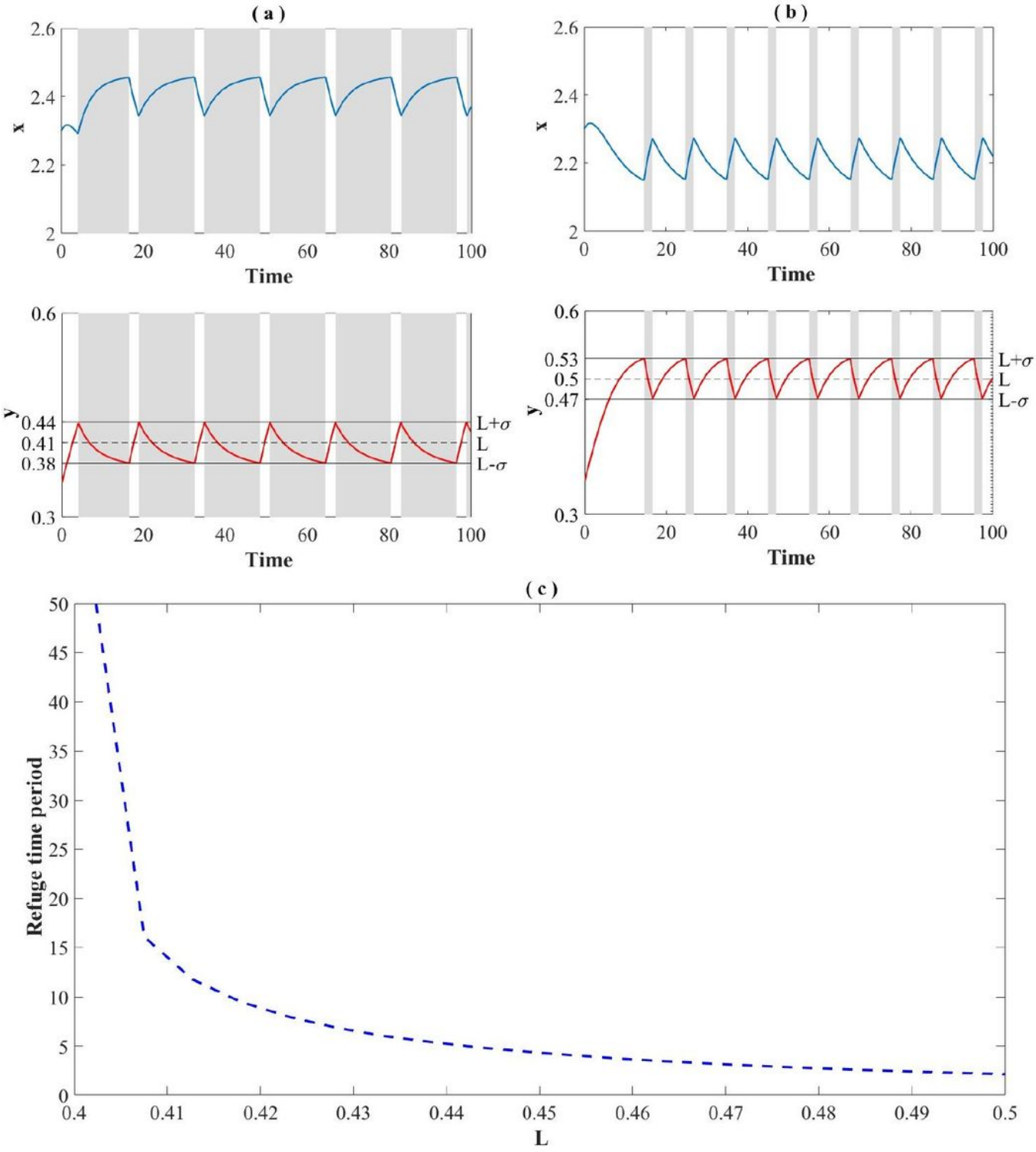

Figure 9

Please see the Manuscript PDF file for the complete figure caption

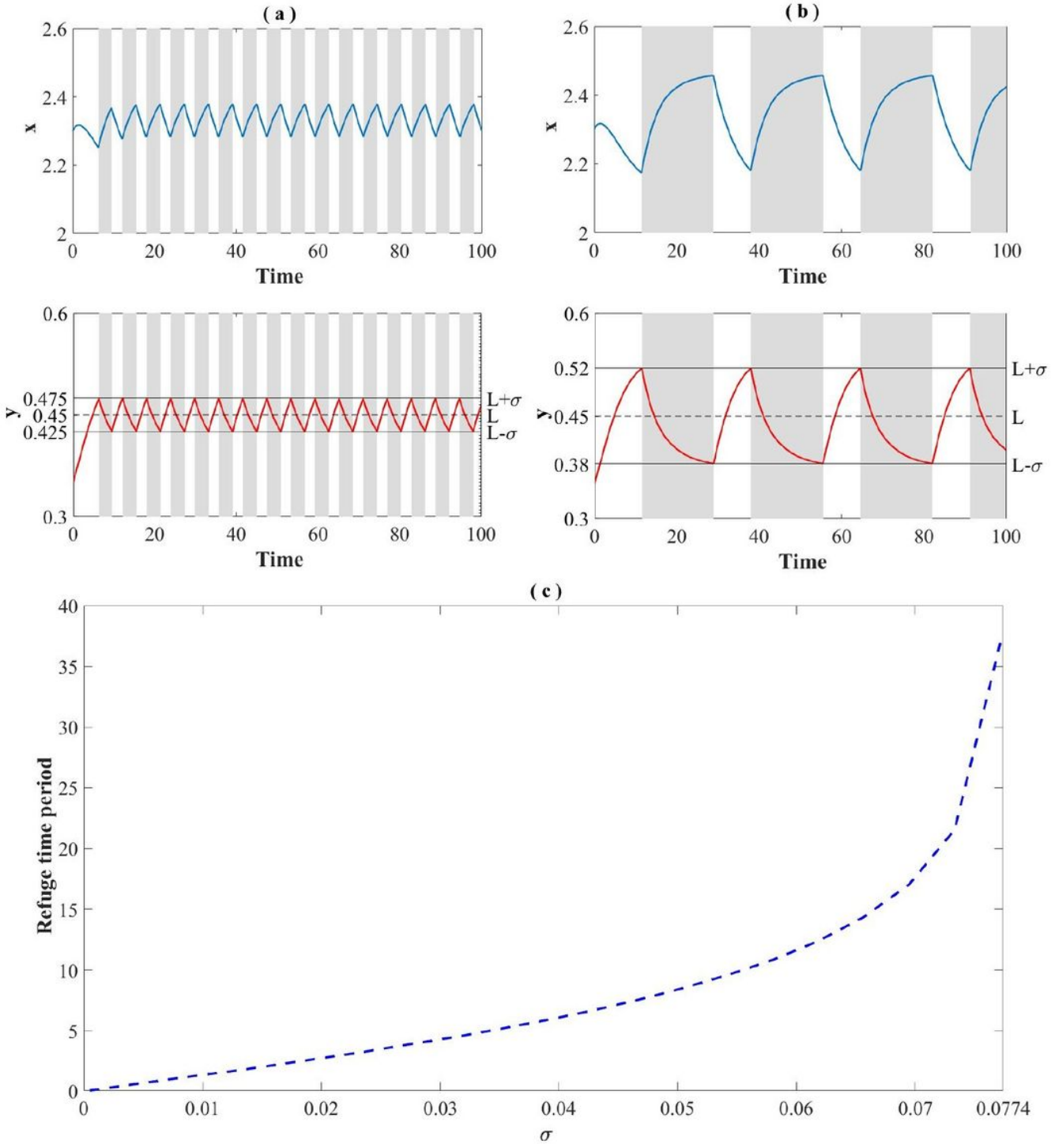

Figure 10

Please see the Manuscript PDF file for the complete figure caption

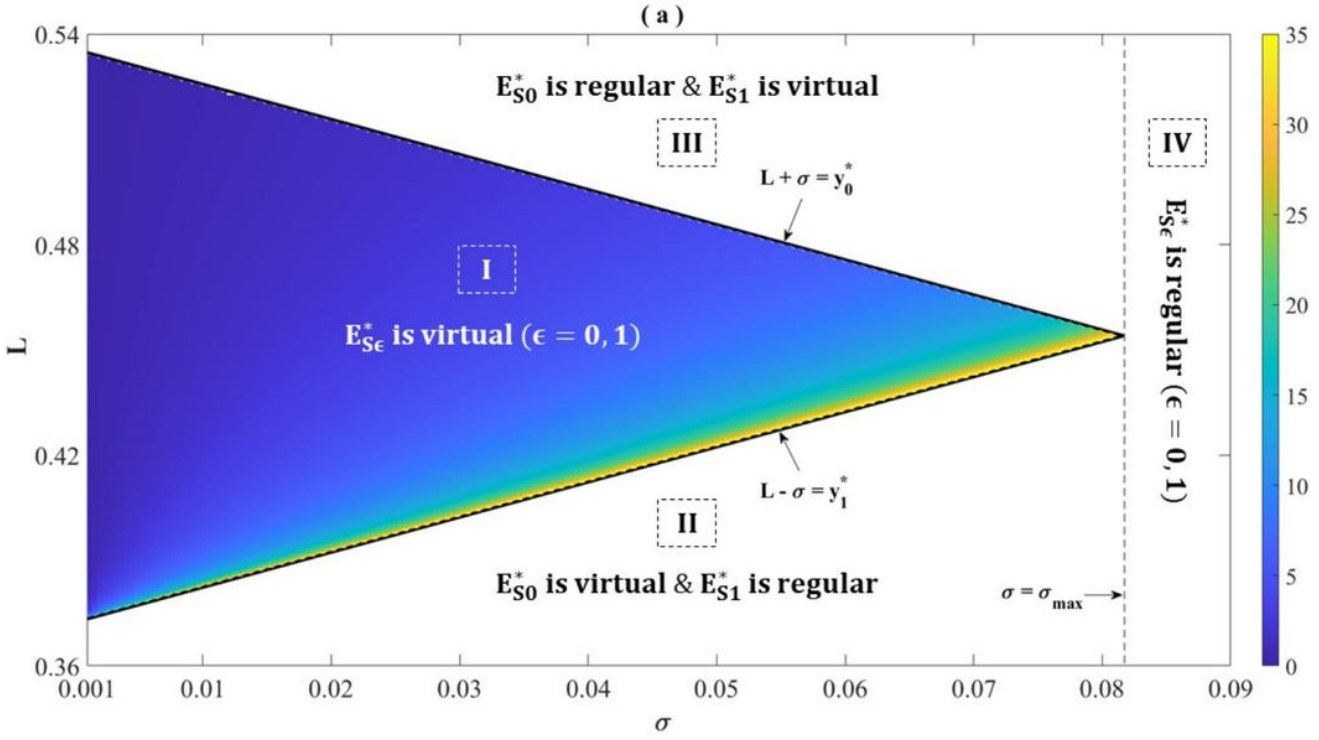

Figure 11

Please see the Manuscript PDF file for the complete figure caption